Univerzita Palackého v Olomouci
Přírodovědecká fakulta
Katedra experimentální fyziky

DIPLOMOVÁ PRÁCE

Optical temperature measurement, the dependence of the effect of emissivity and measurement methods

Autor:	Jan Smolka
Studijní program:	N1701 Fyzika
Studijní obor:	Aplikovaná fyzika
Forma studia:	Prezenční
Vedoucí práce:	RNDr. Tomáš Rössler, Ph.D.
Termín odevzdání práce:	2.6.2020

Prohlašuji, že jsem předloženou diplomovou práci vypracoval samostatně pod vedením RNDr. Tomáše Rösslera, Ph.D., a že jsem použil zdrojů, které cituji a uvádím v seznamu.

V Olomouci dne 2.6.2020 ...…….....

Jan Smolka

Děkuji RNDr. Tomáši Rosslerovi, Ph.D. za kvalifikované vedení mé diplomové práce, cenné rady, zkoušenosti a odbornou pomoc, kterou mi věnoval.

Bibliografická identifikace:

Jméno a příjmení autora	Jan Smolka
Název práce	Optické měření teploty, závislost vlivu emisivity a metody měření
Typ práce	Diplomová
Pracoviště	Katedra experimentální fyziky
Vedoucí práce	RNDr. Tomáš Rössler, Ph.D..
Rok obhajoby práce	2020
Abstrakt	Práce se zabývá problematikou měření teploty v podmínkách průmyslové praxe s důrazem na možnosti bezkontaktního měření teploty. Cílem práce je rozbor měření teploty v rámci konkrétního automatizovaného procesu tepelného lisování ocelové tyče a trubky na polotovar určený k dalšímu zpracování. Výsledkem je hlubší pochopení problematiky takového měření, které je podmínkou pro následnou optimalizaci celého výrobního procesu v rámci zavedeného systému jakosti pracoviště.
Klíčová slova	temperature measurement, emissivity, non-contact measurement, industrial environment
Počet stran	66
Počet příloh	0
Jazyk	Anglický

Bibliographical identification:

Autor's first name and surname	Jan Smolka
Title	Optical temperature measurement, the dependence of the effect of emissivity and measurement methods
Type of thesis	Diplomová
Department	Katedra experimentální fyziky
Supervisor	RNDr. Tomáš Rössler, Ph.D..
The year of presentation	2020
Abstract	This work investigates the problem of temperature measurement in an industrial environment with an emphasis on the possibility of non-contact temperature measurement. The aim of the work is the analysis of temperature measurement within a specific automated process of heat pressing of a steel rod and a tube into a semi-finished product intended for further processing. The result is a deeper understanding of the issue of such measurement, which is a condition for the subsequent optimization of the entire production process within the established workplace quality system.
Keywords	temperature measurement, emissivity, non-contact measurement, industrial environment
Number of pages	66
Number of appendices	0
Language	English

Table of content

1 Introduction

Temperature affects us every day from cold tea to the weather. We are dependent on temperature and to get the right temperature, and it needs to be measured. For the right measurement, it is needed to have the right tools. Choosing the right measuring device takes a little bit to afford because it needs to choose the right devices that will work for measurement. That means select right measuring range, sensitivity and others specifies. Also, not all devices will work in all type of conditions. All these parameters are vital to keeping on mind during the planning and designing an experiment or measuring system.

Temperature measurements are essential in many disciplines. This work is focused on the industrial environment. This measurement is particular, and in own way, it is also unique. In industry, the environment is used almost all kinds of devices for contact or non-contact measurement. It is essential to know how these devices use and for which situation are crucial. For all kind of measurements, it is crucial to get a precise result. The precision is affected by many factors such as the internal temperature of the device, used equipment, conditions and others. The precision in the industrial environment is often lower because it is not necessary to know the precise value and often is not even possible. Also, in some cases, the values are high so ten per cent measurement uncertainty it is unimportant. However, there are some disciplines find in an industrial environment where is needed a precise measurement. If we want to have a more precise measurement, we need to learn about measuring setup and data acquisition.

This work will focus on temperature measurement in an industrial environment, especially on emissivity. Here will be described how emissivity affects measurement and how it can differ for different objects but also comparing different measuring devices during a measurement.

2 Radiation

Maxwell describes radiation as an accelerated charge which creates an electric and magnetic field that correlate to each other. This system moves in the form of a wave with finite speed. This is known as electromagnetic (em) radiation velocity v and can be described as [1]:

$$v = \frac{1}{\sqrt{(\mu\epsilon)}}, \tag{1}$$

where μ is permeability and ϵ is permittivity.

In vacuum

$$v = \frac{1}{\sqrt{(\mu_0\epsilon_0)}} = 3 \cdot 10^8, \tag{2}$$

where is μ_0 is permeability and ϵ_0 is permittivity in vacuum [1].

On the surface, the radiation consists of three parts – reflected, absorbed, transmitted. This can be described from conservation of energy as:

$$Q = Q_a + Q_r + Q_t, \tag{3}$$

where Q is the total radiated energy, Q_a is absorbed energy, Q_r is reflected energy, Q_t is transmitted energy. This can also be described as [1]:

$$1 = a + r + t, \tag{4}$$

where a is absorption

$$a = \frac{Q_a}{Q}, \tag{5}$$

r is reflection

$$r = \frac{Q_r}{Q}, \tag{6}$$

t is transmission

$$t = \frac{Q_t}{Q}. \tag{7}$$

Non-contact temperature measurement, also known as thermography, uses infrared radiation (IR). IR is described as the range of wavelength λ = 0.75 μm – 1 mm. This allows measurement in the range of temperatures from - 40 °C to 10^3 °C. IR is divided as [2]:

- Near-Infrared (NIR), λ = (0.75 – 1.4) μm [2].
- Short Wavelenght Infrared (SWIR), λ = (1.4 – 3) μm [2].
- Mid Wavelenght Infrared (NWIR), λ = (3 – 5) μm [2].
- Long Wavelenght Infrared (LWIR), λ = (5 – 15) μm [2].
- Far Infrared (FIR), λ = 15 μm – 1 mm [2].

Radiation energy in the infrared spectrum can be generated by three sources – luminescent, radio, heat. Thermography is an essential source of heat. Body surfaces are heated by absorption of electromagnetic light. For example, objects in room temperature emit radiation in the range of wavelengths from 8 μm to 12 μm. For heat source is typical that the heat energy of a source covers generated radiation energy. This means the whole body generates IR radiation. His temperature is higher than absolute zero (T > 0K). Amount of radiant flux generated heat sources, his spectral distribution and direction of propagation depend on properties source of heat. Radiant flux is represented as photon flux in the IR spectrum. This spectrum can be described by using the Black body or grey body [2].

2.1 Kirchhoff law

In 1860 Kirchhoff deduced the fraction of radiation intensity $I(T)$ and absorption $\alpha(T)$ of the body does not depend on the material but on specific temperature function that is written as [3]

$$\frac{I(T)}{\alpha(T)} = f(T). \tag{8}$$

This law says the amount of absorbed energy is proportional to radiated energy. This fact must be fulfilled for all range of wavelengths λ and it can be written as [3]

$$\frac{I(T,\lambda)}{\alpha(T,\lambda)} = f(T,\lambda), \tag{9}$$

Because also $\alpha(T,\lambda)$ is proportional to $I(T,\lambda)$ that means a higher $\alpha(T,\lambda)$ is higher $I(T,\lambda)$. The most absorbed wavelength is the most radiated wavelength [3].

The absorption coefficient for bb is $\alpha(T,\lambda) = 1$. This conclusion can be applied to Kirchhoff law that can be written as [3]

$$f(T) = I_0(T) \tag{10}$$

(11)

$$f(T,\lambda) = I_0(T,\lambda).$$

For multiple intensity H radiation at the same temperature conditions can be applied [3]

$$I_0(T,\lambda) = \frac{I_1(T,\lambda)}{\alpha_1(T,\lambda)} = \frac{H_2(T,\lambda)}{\alpha_2(T,\lambda)} = \cdots \frac{H_3(T,\lambda)}{\alpha_3(T,\lambda)} \tag{12}$$

Where indexes indicate a different type of material. In terms of emissivity ε, it can be written as [3]

$$I(T,\lambda,\varepsilon(T,\lambda)) = \varepsilon(T,\lambda) \cdot H_0(T,\lambda). \tag{13}$$

2.2 Black Body

A black body (bb) is described as the ideal body that absorbs radiation ideally without passing and reflecting the energy. 3

That means if bb is heated and kept at a fixed temperature, then radiation is partially reflected and absorbed into walls of bb (shown in Fig. 1). This property works on all radiation spectrum and for all angles. When is cavity is filled by radiation, the temperature of bb is fixed, and radiation is in thermal equilibrium. In other words, it means the quantity emitted radiation (per sec) is the same quantity absorbed. Black body applies a = 1, r = t= 0 [1].

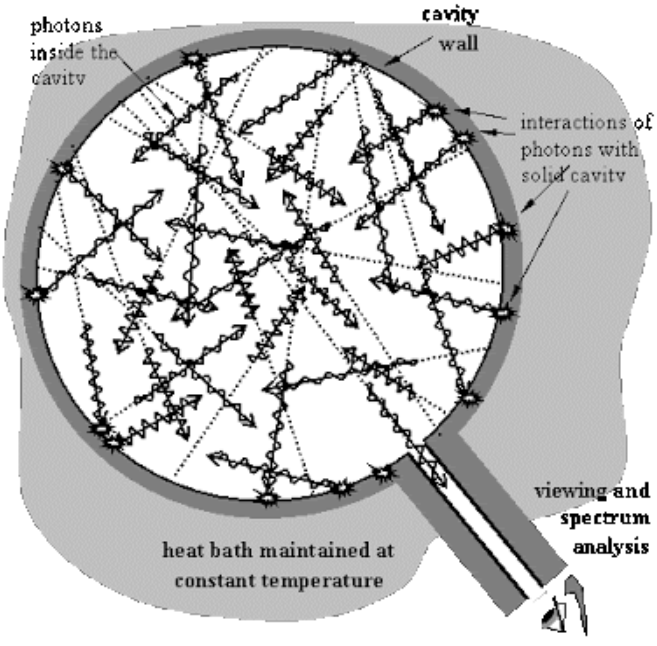

Fig. 1: Model of a black body. Taken from [4]

For experiments, it can approximate bb as a hollow body with a tiny aperture. All radiation comes thru aperture to the body, stays in it and become absorbed by walls of bb.

Walls of the body absorbs and emits radiation. It can be only studied radiation that comes out form body aperture. This emitted radiation has higher energy with higher temperature. It was experimentally found amount energy of radiation that depends on wavelength λ change with temperature [6].

Due to Kirchhoff's law (described in chapter 2.1) the emissivity and absorption are equal [13]

$$\varepsilon(\lambda, T) = a(\lambda, T). \tag{14}$$

The (4) equation can be rewritten as

$$1 = \varepsilon + r + t. \tag{15}$$

2.3 Planck's law

Planck's law describes bb radiation. Let assume photon with zero invariant mass $m_0 = 0$, energy is defined as [3]:

$$E = hf = \hbar\omega \tag{17}$$

and momentum [3]

$$p = \frac{E}{c} = \frac{\omega}{c}\hbar = \frac{2\pi}{\hbar}, \tag{18}$$

where c is the speed of light, h is Planck's constant, ħ is reduced Planck's constant, ω angular frequency. Photons as bosons obey Bose-Einstein (B-E) distribution that gives us an expected number of particles in an energy state. The expected value $n(\omega)$ of particles in an energy state for B-E is defined as [3]

$$n(\omega) = \frac{1}{e^{\left(\frac{\hbar\omega}{kT}\right)} - 1}, \tag{19}$$

Where k = 1.38064852 × 10^{-23} m^2 kg s^{-2} K^{-1} is Boltzman constant, T is the temperature in Kelvins. The volume of phase space corresponding to energies (0, E) of a photon is defined as [3]:

$$\Gamma(E) = V\Gamma_p(E) = V\frac{4}{3}\pi\left(\frac{E}{c}\right)^3, \tag{20}$$

where $\Gamma_p(E)$ is the volume of momentum part of phase space that is defined as the sphere with radius $p = \frac{E}{c}$. Number of states with energies between $(0.E)$ is equal [3]

$$\Gamma(E) = 2\frac{\Gamma(E)}{(2\pi\hbar)^3} = \frac{VE^3}{3\pi^2c^3\hbar^3}, \tag{21}$$

where $\frac{\Gamma(E)}{(2\pi\hbar)^3}$ is multiplied by 2, because photons have two polarisations and each state have twice degenerated [3].

For the density of degeneration $g(E)$ is defined as the number of states with energy E on a layer with width $\mathrm{d}E$ on the surface of a sphere of radius, R is equal [3]

$$g(E)dE = \frac{\mathrm{d}\Gamma}{\mathrm{d}E}\mathrm{d}E = \frac{V}{\pi^2 c^3 \hbar^3} E^2 \mathrm{d}E, \tag{22}$$

where $\frac{E}{h}$, $\frac{1}{\hbar}\mathrm{d}E$ is equal to $\omega = \frac{E}{\hbar}$, $\mathrm{d}\omega = \frac{1}{\hbar}\mathrm{d}E$ thanks to this we get

$$g(\omega) = \frac{V}{\pi^2 c^3}\omega^2 \tag{23}$$

This gives us an amount of photon that has a frequency in the interval $[\omega, \omega + d\omega]$:

$$g(\omega)n(\omega) = \frac{V}{\pi^2 c^3}\omega^2 \frac{1}{e^{\left(\frac{\hbar\omega}{kT}\right)} - 1}. \tag{24}$$

For getting energy density $\rho(w)$that corresponds to frequency ω [3].

$$\rho(w)d\omega = \hbar\omega n(\omega)g(\omega) = \hbar\omega \frac{\omega^2}{\pi^2 c^3} \frac{1}{e^{\left(\frac{\hbar\omega}{kT}\right)} - 1} d\omega. \tag{25}$$

From (16) we get Planck's radiation law [3]

$$\rho(\omega) = \frac{\hbar}{\pi^2 c^3} \frac{\omega^3}{e^{\left(\frac{\hbar\omega}{kT}\right)} - 1}. \tag{26}$$

Two-dimensional plot of Planck's law for different temperatures can be seen in Fig. 2

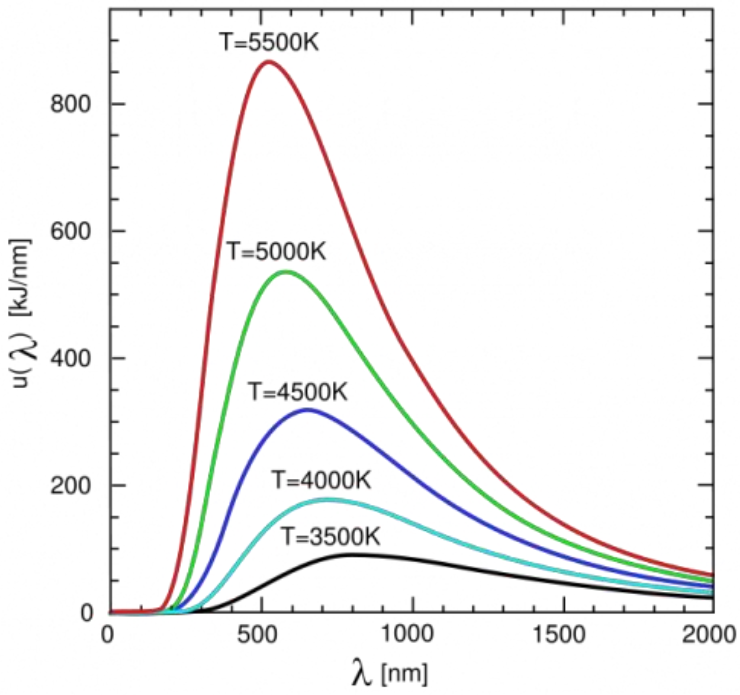

Fig. 2: Two-dimensional plot of Planck's law for different temperatures. Taken from [7]

2.4 Wien's Displacement law

Wilhelm Carl Werner Otto Fritz Wien won a Nobel prize in 1911 for discovery temperature and wavelength dependence. It is defined as [8]:

$$\lambda_p T = 2.8978 \cdot 10^{-3}\ [\mathrm{m} \cdot \mathrm{K}], \tag{27}$$

where λ_p is peak wavelength and T is the absolute temperature [8]. The wavelength dependence can be seen in Fig.4.

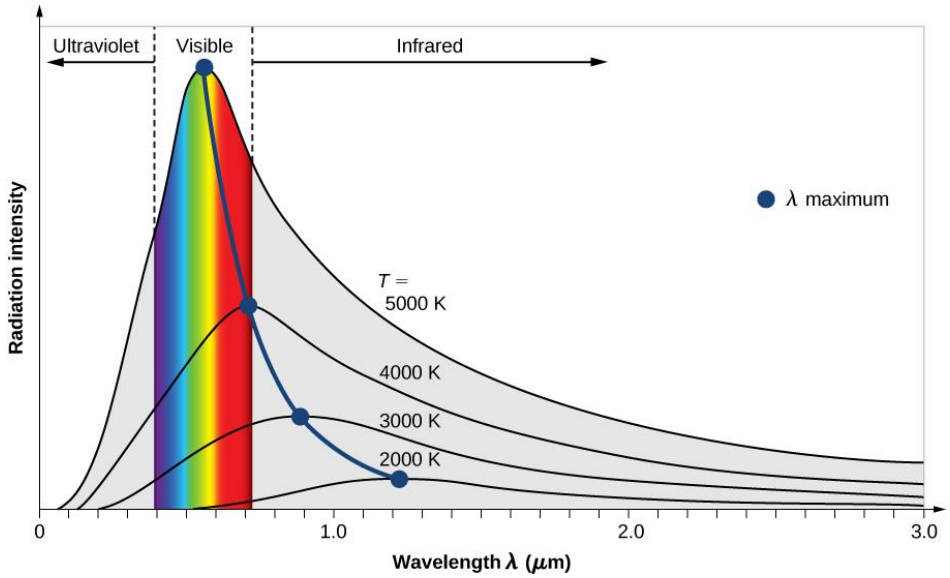

Fig. 3: Two-dimensional plot of Planck's law with peak wavelengths (blue dots) for different temperatures. Taken from [9]

2.5 Stefan – Boltzmann law

Later in 1884, this law was derived by Boltzmann [3]. Stefan-Boltzmann law was got without any knowledge on the spectral repartition of black body emission. For Boltzmann's derivation it is necessary to use the entropy $S(U,V)$. An infinitesimal transformation is an entropy described as:

$$TdS = dU + pdV = \frac{\partial U}{\partial T}\, dT + \left(p + \frac{dU}{dV}\right) dV, \tag{28}$$

because entropy is total differential it leads to

$$\frac{\partial p}{\partial T} = \frac{p+u}{T}, \tag{29}$$

by using Maxwell-Boltzmann relation $p(T) = \frac{u(T)}{3}$ we can assume:

$$\frac{1}{4}\frac{du}{u} = \frac{dT}{T} \tag{30}$$

This leads to Stefan law

$$u(T) = \sigma T^4 = \frac{\pi^2 k_b^2}{15\hbar^2 c^3} T^4, \tag{31}$$

where $u = \frac{U}{V}$,k_b is Boltzmann constant, T is temperature.

2.6 Emissivity

The emissivity is a material property that gives us information about how much surface can emit thermal radiation. This knowledge is needed, for example, in the spacecraft industry or thermal measurement [10].

The emissivity of real objects ε_r is described as:

$$\varepsilon_r = \frac{I_\lambda}{I_{\lambda b}}, \tag{32}$$

where I_λ is the intensity of real object , $I_{\lambda b}$ is the intensity of bb at the same temperature and at the same wavelength as real object [11].

If an object does not change their emissivity with the wavelength, it is known as greybody. In Fig.5 is displayed a comparison between bb, greybody and the real object.

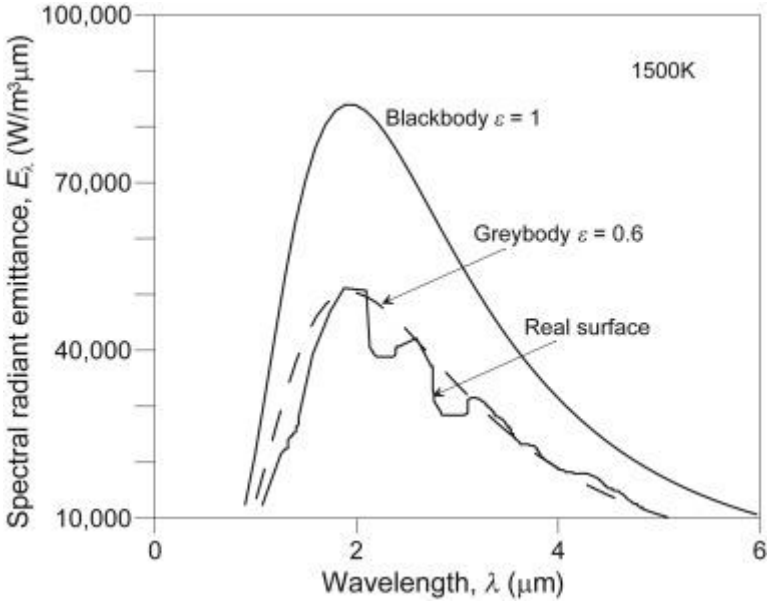

Fig. 4: Comparison between bb, greybody and the real object. Taken from [11].

From Fig. 4 it is noticeable that the radiation curve of bb and greybody are the same but scaled-down, because of different emissivity [11].

It can also be defined as real Stefan- Boltzmann law with emissivity ε dependence as [2]:

$$u(T) = \varepsilon\sigma T^4. \tag{33}$$

Two-dimensional plot for real Stefan- Boltzmann law with difference emissivity can be seen in Fig. 5.

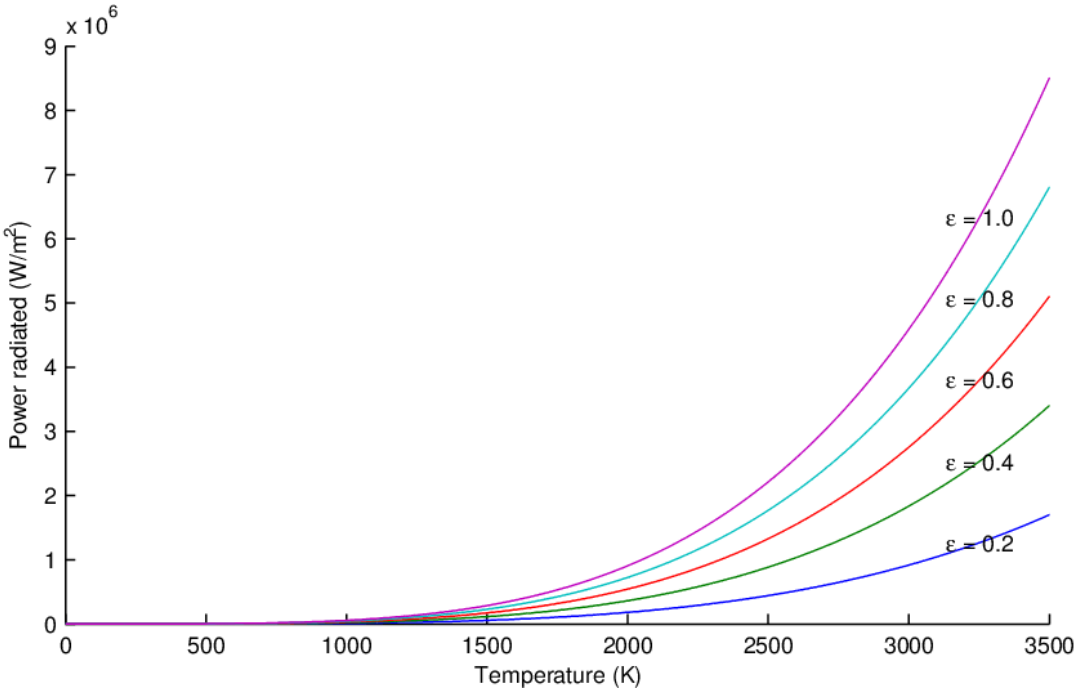

Fig. 5: Two-dimensional plot for real Stefan-Boltzmann law with difference emissivity values. Taken from [2]..

2.7 Pseudotemperatures

Pseudotemperatures come from radiation intensity of measured surface and BB. Assume the radiation of bb a measured body is at same temperature T. Kirchhoff's law defines $I_0(T_0) \geq I(T)$ and gives us a formula [3]

$$\frac{I(T)}{I_0(T)} = \varepsilon(T). \tag{34}$$

In case when $I_0(T_0) = I(T)$ the temperatures will not be the same ($T_0 \neq T$). Kirchoff's law defines $T_0 > T$, the T_0 is called pseudo temperature, and it is defined as the temperature of bb when the radiation intensity of bb $I_0(T_0)$ is equal to radiation intensity of radiator $I(T)$ [3].

3 Temperature measurement

The systems for thermal measurement can be divided into two groups. The first group is the contact measurement. The contact measurement arises when there is physical contact between the measuring device and the measured object. The second group is the non-contact measurement. The main difference between the first group is that between measuring device and measured object is not physical contact. The non-contact measurement is always used in the situation when we are dealing with a higher temperature that could damage the contact measuring device or with moving objects. We can often see non-contact measuring in medicine, where doctors measure body temperature or in metallurgic companies where they are dealing with really high temperatures [12].

3.1 Units of temperature and ITS90

There are two central units of measurement of temperature that we mostly use: kelvins, degrees of Celsius [13].

Degree of Kelvin is defined by the triple point of water and Boltzmann constant *k*. The Boltzmann constant and triple point of water are defined by Bureau International des Poids et Mesures (The International Bureau of Weights and Measures – BIPM) [14]. The Celsius degree is defined by Kelvin temperature as:

$$t = T - 217.5, \tag{35}$$

where t is a temperature in Celsius, T is a temperature in Kelvins [13].

3.1.1 The International Temperature Scale of 1990

The International Temperature Scale of 1990 (ITS90) was adopted in 1989 by the International Committee of Weights and Measures due to accordance with the request from the 18th General Conference of Weights and Measures in 1987.

ITS.90 has three primary definitions. The first definition is for temperature between 0.65 K and 5.0 K for ^{3}He and ^{4}He in vapour-pressure relations. The second definition is for temperature between 3.0 K and 24.5561 K (triple point of neon) where is used helium gas thermometer that is calibrated for three fixed points of temperature. The third definition is for temperature between 13.8033 (triple point of equilibrium hydrogen) and 1235 K (freezing point of silver) where is used platinum resistance thermometer that is calibrated at defining fixed points [13].

3.1 Contact measuring devices

The contact measuring device can be made from epoxy, glass or stainless steel or particular metal that have given thermal conductivity properties. We can find these devices in different forms as rods, beads and probes. The size of the sensor can be small as 0.1 mm in diameter due to short response time. Those devices we call resistance temperature devices (RTD) [16]

3.1.1 Thermistor

The first type of contact measuring devices is resistance thermometers that are measuring temperature based on changes in electrical resistance of the sensor. Two types of resistance thermometers are mostly used. The first type is the thermistors. A sensing element of a thermistor is a semiconductor. The semiconductor is made of from metallic oxides. The resistance of metallic oxide decreases as the temperature of object increases. This can be described as

$$R = R_0 \cdot e^{b\left(\frac{1}{T}-\frac{1}{T_0}\right)}, \tag{36}$$

where R is electrical resistance in Ohms [Ω] at given temperature T in Kelvins [K], R_0 is referencing electrical resistance in Ohms for reference temperature T_0 in Kelvins. The reference temperature T_0 is usually given for room temperature (298 K or 25°C). For specific materials is given a constant b. The manufacturer always gives the reference temperature and constant b in the datasheet [16].

3.1.2. Resistance thermometers

The second type is resistance thermometers. The sensor of RTD is made of metal materials (platinum, nickel, copper), and this specific metal has given thermal conductivity properties that we can measure as electrical resistance. This can be described as

(37)

$$R_T = R_0(1 + \alpha T + \beta T_2 + \gamma T_3 + \ldots),$$

where R_T is the electrical resistance in Ohms [Ω] at given temperature T, R_0 is referencing electrical resistance in Ohms (Ω) for the reference temperature T_0 in Kelvins [K], and α, β, γ are material constants. The reference temperature T_0 usually given for 273.15 K (0°C).

The most used material for RTD sensor is platinum. The corresponding temperature at 0°C and 100°C is usually 100Ω and 139Ω. The precise measurement also depends on lead wire resistance and temperature changes in the lead wire that could cause significant changes in resistance readings [16]. A most used one is Pt100, as shown in Fig 6.

Fig. 6: Resistance thermometer Pt100. Taken from [18]

3.2 Non-contact measuring devices

Non-contact thermometers use different physical principles to get the temperature of an object. These principles are radiation phenomenon, refraction, Doppler effect, luminescence and others.

3.2.1. Thermocouples

Thermocouples are widely used for measuring temperature because they are robustness, cheap, and they have a large temperature range. A thermocouple is made from two different wires (shown in Fig.7).

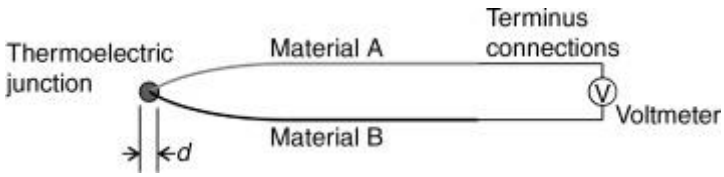

Fig. 7: Scheme of a thermocouple. Taken from [19]

It can be measured small current if the temperature is different at the junction. This was discovered by Thomas Johann Seebeck in 1823 [20].

3.2.1.3 Seebeck effect

A thermocouple is based on the Seebeck effect. Seebeck effect is caused by electromotive force (EMF) in the junction of two different conducting materials, where two junctions are connected and hold two different temperatures T and T_{REF}. By that, we can measure EMF voltage V between their free contacts. This given by the formula

$$V = S(T - T_{REF}), \tag{38}$$

where S is the Seebeck coefficient in $V \cdot °C^{-1}$ [20] , we can transform this formula as

$$T = T_{REF} + \frac{V}{S}. \tag{39}$$

A special voltmeter measures the output voltage. For precision measurement reference junction should be kept in a triple point of water in a fixed temperature of 0.01 + 0.0005 °C. Still, the reference is usually can be room temperature [16]. The formula for contact potential V_c can be formulated as:

$$V_c = \left(\frac{kT}{e}\right) \ln\left(\frac{n_L}{n_r}\right), \tag{40}$$

where k is Boltzmann constant, T is absolute temperature, e is the electron charge and n_L is left higher density, n_R is right lower density. In Fig. 7 is shown types of thermocouples.

Type	Alloy	Temperature	Standard Limits	Special Limits
T	Copper (+) vs. Constantan (–)	–200°C to 0°C* 0°C to 350°C	±1°C or ±1.5%* ±1°C or ±0.75%	±0.5°C or ±0.8%* ±0.5°C or ±0.4%
J	Iron (+) vs. Constantan (–)	0°C to 750°C	±2.2°C or ±0.75%	±1.1°C or ±0.4%
E	Chromel®(+) vs.Constantan (–)	–200°C to 0°C* 0°C to 900°C	±1.7°C or ±1%* ±1.7°C or ±0.5%	±1°C or ±0.5%* ±1°C or ±0.4%
K	Chromel® (+) vs. Alumel®(–)	–200°C to 0°C* 0°C to 1250°C	±2.2°C or ±2%* ±2.2°C or ±0.75%	N.A. ±1.1°C or ±0.4%
N	Nicrosil (+) vs. Nisil (–)	0°C to 1250°C	±2.2°C or ±0.75%	±1.1°C or ±0.4%
R	Pt/13%Rh (+) vs. Pt (–)	0°C to 1450°C	±1.5°C or ±0.25%	±0.6°C or ±0.1%
S	Pt/10%Rh (+) vs. Pt (–)	0°C to 1450°C	±1.5°C or ±0.25%	±0.6°C or ±0.1%
B	Pt/30%Rh (+) vs. Pt/6%Rh (–)	870°C to 1700°C	±0.5%	±0.25%

Fig. 7: Types of thermocouples with temperature ranges and their limits. Taken from [21].

3.2.1.1 Thompson effect

Thompson effect describes the absorption or production of a heated conductor, where temperature gradient ΔT is dependent on an electric charge that flows through a conductor. The heat that Is created or absorbed in a conductor segment can be described as [18]:

$$\frac{dQ}{dt} = -K_2 J \Delta T, \tag{41}$$

where J is a current density, K_2 is second Thompson's coefficient. There are two main Thompson's coefficients. First is characterised as [18]: (42)

$$K_1 = T S_B,$$

where T is the absolute temperature and S_B is the Seebeck coefficient. The second coefficient is described as [20]:

$$K_2 = T \frac{dS}{dT}. \tag{43}$$

There are certain types of thermocouples. It depends on the usage and types of used alloys. The types are stated in Fig. 7.

3.2.1.1 Peltier effect

Peltier effect uses electrical work from a power source that is converted in a junction to thermal heat. This is achieved by an acceleration of charge carriers in the electric field. Electrons are

(44)

slowed or accelerated by potential difference, that depends on the direction of the velocity vector depend on the electrical field. The amount of heat produced or absorbed at the junction between A and B conductors can be described as [20]:

$$\frac{dQ}{dt} = (\Pi_A - \Pi_B)I,$$

Where I is the electric current and Π_A , Π_B are Peltier coefficients for A, B conductor. These coefficients are described as [20]:

$$\Pi_A = kTln(n_L) \tag{45}$$

And

$$\Pi_B = kTln(n_R), \tag{46}$$

where k is Boltzmann constant, T is the absolute temperature and n_L is left higher density, n_R is right lower density [20].

3.2.1.4 Output voltage

The electromotive force (emf) of a thermocouple is given by power series [22]:

$$V\ [mV] = (A\delta + B\delta^2 + C\delta^3..) - (A\delta_0 + B\delta_0^2 + C\delta_0^3..), \tag{47}$$

where A, B, C are characteristic constants for used metals of thermocouple, δ, δ_0 are temperatures held by junctions. The δ held higher temperature and δ_0 held lower temperature. Often is used $\delta = 100\ °C$ and $\delta_0 = 0\ °C$ [22]. For conversion from thermocouple voltage V (in mV) to temperature t is used formula [23]:

$$t = d_0 + d_1V + d_2V^2 + .. + d_nV^n, \tag{48}$$

where d is voltage range for K-type thermocouple that can be found in Fig.7.

Temperature Range:	−200°C to 0°C	0°C to 500°C	500°C to 1372°C
Voltage Range	−5891 µV to 0 µV	0 µV to 20644 µV	20644 µV to 54886 µV
d_0	0.000 000 0	0.000 000 0	$-1.318\ 058 \times 10^{2}$
d_1	$2.517\ 346\ 2 \times 10^{-2}$	$508\ 355 \times 10^{-2}$	$4.830\ 222 \times 10^{-2}$
d_2	$-1.166\ 287\ 8 \times 10^{-6}$	$7.860\ 106 \times 10^{-8}$	$-1.646\ 031 \times 10^{-6}$
d_3	$-1.083\ 363\ 8 \times 10^{-9}$	$-2.503\ 131 \times 10^{-10}$	$5.464\ 731 \times 10^{-11}$
d_4	$-8.977\ 354\ 0 \times 10^{-13}$	$8.315\ 270 \times 10^{-14}$	$-9.650\ 715 \times 10^{-16}$
d_5	$-3.734\ 237\ 7 \times 10^{-16}$	$-1.228\ 034 \times 10^{-17}$	$8.802\ 193 \times 10^{-21}$
d_6	$-8.663\ 264\ 3 \times 10^{-20}$	$9.804\ 036 \times 10^{-22}$	$-3.110\ 810 \times 10^{-26}$
d_7	$-1.045\ 059\ 8 \times 10^{-23}$	$-4.413\ 030 \times 10^{-26}$	
d_8	$-5.192\ 057\ 7 \times 10^{-29}$	$1.057\ 734 \times 10^{-30}$	
d_9		$-1.052\ 755 \times 10^{-35}$	
Error Range	0.04°C to −0.02°C	0.04°C to −0.05°C	0.06°C to −0.05°C

Fig. 8: Temperature coefficients for K-type thermocouple according to ITS-90. Taken from [23]

3.3.1. Pyrometers

We can find pyrometers widely in many areas like metallurgy, chemical development and at other manufactures areas. They can be used for measurements of moving objects, can access to difficult places or objects located in high-temperature areas where is a high potential risk for workers [24].

In an ideal theoretical case, all materials emitted the same amount of light and at the same temperature. To determine the amount of light is called emissivity. Emissivity is how efficient each material emits light. In the ideal case, the emissivity is equal to one. In other cases is emissivity below one (the emissivity is described in the chapter) [25].

We can divide pyrometers into two types. The first type is one colour pyrometer. These pyrometers convert light into the temperature – the higher amount of light pyrometer gets and the higher temperature it measures. This depends on the material's emissivity and must be known for correct measurement. If huge temperature errors occur during measurement, it is mostly caused by the incorrect setting of emissivity. The second type is two-colour pyrometer. These pyrometers consist of two detectors to capture different wavelengths. The division amount captured light by each detector, give us a temperature. It also depends on emissivity but in ideal cases is emissivity at the same wavelength and cancels out in that division. In case of metal are not ideal for measurement. The emissivity of metal changes fasts with their wavelengths. For this case, the ratio pyrometer causes difficulty. For measurement, it is important to know the non-greyness or relative emissivity. The special type of pyrometer is multi-wavelengths pyrometers also call Spectro Pyrometers. This device can measure at hundreds of wavelengths and can sense all data, that captures from different wavelengths and can determine more information than just temperature [25].

Another way how to divide pyrometers type of measurement

- Total radiation pyrometers - They use a principle of SB-law. This evaluates temperature from $\lambda = 0$ to $\lambda = \infty$ but spectral absorption of the detector is never ideal, and the range of λ is limited. Usually the limitation is from $\lambda = 0{,}4\ \mu m$ to $\lambda = 20\ \mu m$. For IR detection is used thermal detector [27].

- Wideband pyrometers – are spectral selective non-contact thermometers. They are using a principle of Wien law. This allows them to measure in a short range of λ. For IR

detection is used microbolometer. The most significant advantage is a short time constant high sensitivity [27].

- Proportional pyrometers – evaluates surface temperature of an object based on a ratio of two radiated intensity for two λs that are calibrated on BB temperature for two λs. This can be proven from Planck's law; the ratio of two intensities is every temperature different and also independent on emissivity. The most significant disadvantage is a sophisticated design and a higher price [27].
- Pyrometers with automatic emissivity correction – They measure the surface temperature of an object without knowledge his emissivity. The principle is based on the wideband measurement and intensity measurement and intensity radiation measurement of an object that is heated by laser with defined radiation intensity [27].

Pyrometer consists of an optical system and signal processing unit (SPU). The optical system is assembled from lens, filter, detector, aperture. In SPU it can be found A/D converter, amplifier, microprocessor.

Heated object radiates infrared photons. This radiation is focused by the lens and going through the aperture and the filter. Aperture removes radiation from edges, and the filter passes only wanted spectral range rays. These rays are captured on the detector. The signal is converted from analogue to digital and amplified. The amplified signal is processed in a microprocessor [28]. The block scheme for pyrometer (same for a thermal camera) can be seen in Fig. 8

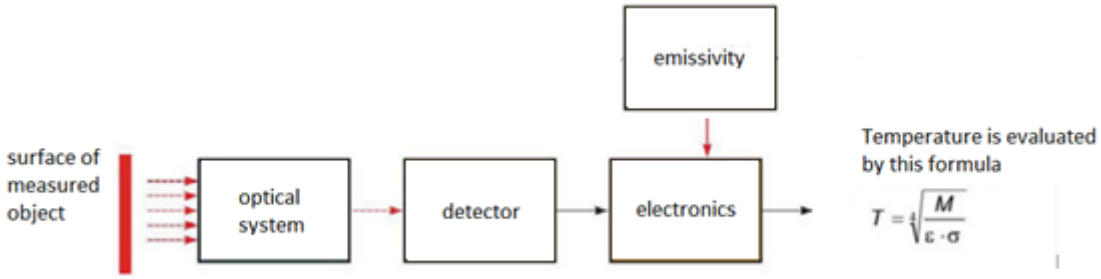

Fig. 9: Block scheme of the pyrometer and thermo-camera. Adopted from [29].

3.3.2 Thermal camera

Thermal imaging camera (TIR) is a non-contact device that uses infrared imaging to display and record temperature across the scanning area of an object. The technique used in TIR is called infrared thermography (IT). The idea of infrared radiation was established in the early 19th century by astronomer William Herschel who discovered a new type of radiation in the spectrum beyond red light. Later in 1929, the Hungarian physicist invented night vision the electronic television camera [31].

Since then, TIRs have become compact size device that produces real-time crisp, high-resolution images. These properties are making them a widely used tool for industrial applications. The main advantage is a non-invasive, non-destructive method to visualise the temperature distribution of an object [32]. Difference between thermal camera pyrometer is shown in Fig.10.

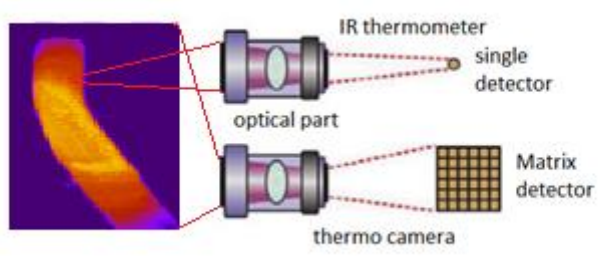

Fig. 10: Comparassion of thermal-camera and IR Thermometer. Adopted from [29].

3.3.2.1 Thermo camera construction

Thermo camera is same as in case of the pyrometer, but it differs in a used sensor. Pyrometer uses bolometer, but TIR uses CCD or CMOS detector. This allows seeing in real time an image with heated areas. Image is completed with pseudo-colours (For example red is hottest, blue is coldest (see Fig. 10) [32].

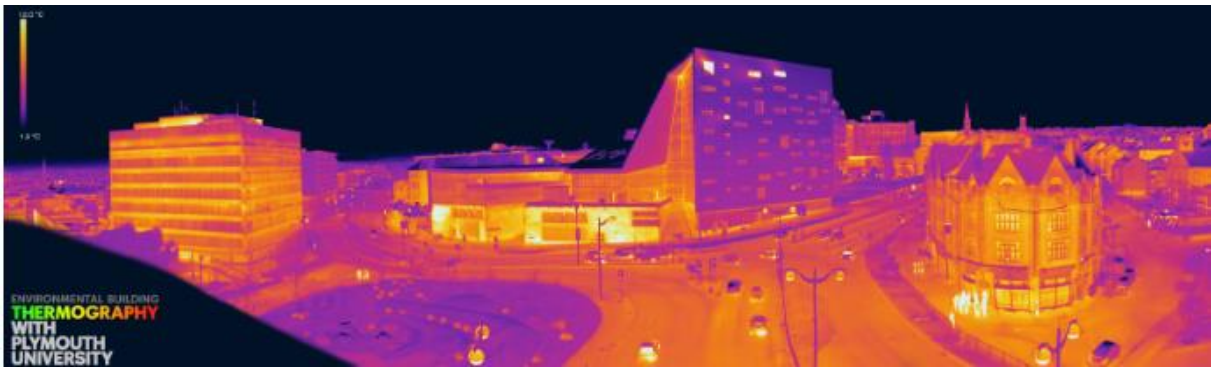

Fig. 11: Thermal image of Plymouth university in pseudo-colours, where purple is coldest and white hottest. Taken from [33]

4 Used equipment

4.1 ThermoImager TIM 160

TIM 160 (T160) is a small thermal imaging camera by Microepsilon (shown in Fig). Its measuring range is from -20 °C to 900 °C. T160 contains exchangeable lenses 6°, 23°, 48°, 72°FOV. It uses a USB 2.0 interface that is used for data transfer and power supply. Via USB 2.0 interface provides real-time thermography with 120 Hz frame rate. The camera is placed in aluminium, anodised housing that provides high ingress protection – IP65.

T160 uses TIM Connect (TC) software developed by Microepsilon that freeware. TC displays a real-time thermal image with a wide range of measurement tools and functions. It can provide analysis and post-process infrared videos or images. TC also provides a complete set up of parameters and remote control of the camera. The interface of TC is shown in Fig. 11 [34].

Fig. 12: ThermoImager TIM 160 by MicroEpsilon. Taken from [35]

4.2 Metis MS09

Metis MS09 (MS09) is pyrometer by Sensotherm. MS09 (shown in Fig. 10) consists of a silicon detector that operates at the near end of the infrared spectrum. MS09 has built a laser aiming light. The aiming light can be focused by optics that is part of the pyrometer. Lenses are made of BK7, an optical glass which is highly transparent in the spectral region of MS09. Detector and optical, electronic parts are housed in an extruded aluminium casing that provides high ingress protection – IP65.

MS09 uses software named Sensorwin. The Sensorwin is free and allows set up of properties of the pyrometer. This can be done automatically or manually—Sensorwin exports data as graphs or text file [36]. The MS09 can be seen in Fig. 12.

Fig.13: Pyrometer Metis MS09 by Sensotherm. Taken from [37]

4.3 Datalogger PhoenixTM HT

Datalogger PhoneixTM HT (shown in Fig. 14) is made for high-temperature applications it has to measure range from 0°C to 1760 °C. This datalogger provides six, ten or twenty channels and has a large variety of options for used thermocouples. It covers types K, N, R, S, B. Datalogger is mounted in IP67 housing. It can be connected via USB or wireless. The wireless method is done via Bluetooth (only PC connection, not for measurement) or radiofrequency system these feature makes data logger more versatile, and it can be used in hardly reachable areas [38].

It has a 0.1 °C resolution and sample interval from 0.2 seconds to 60 minutes. The datalogger operates via Thermal View Plus. Thermal View Plus is a simple software, but powerful software to create specific settings for measurement and capturing data [38], for measurements was used

K-type thermocouple. Used was from 500 °C to 1000 °C, the specification can be seen in Fig. 15.

Fig. 14: Datalloger Phoenix, a version PTM1220. Taken from [39]

Temperature Range:	500°C to 1372°C
Voltage Range	20644 µV to 54886 µV
d_0	$-1.318\ 058 \times 10^{2}$
d_1	$4.830\ 222 \times 10^{-2}$
d_2	$-1.646\ 031 \times 10^{-6}$
d_3	$5.464\ 731 \times 10^{-11}$
d_4	$-9.650\ 715 \times 10^{-16}$
d_5	$8.802\ 193 \times 10^{-21}$
d_6	$-3.110\ 810 \times 10^{-26}$
d_7	
d_8	
d_9	
Error Range	0.06°C to –0.05°C

Fig. 15: Used specification for T-type thermocouple. Adopted from [23].

5 Data evaluation

5.1 Operational temperature measurement

5.1.1 Introduction

The manufacturing process uses three measuring devices – two pyrometers and one thermal camera. The pyrometers measure the temperature of an object that was heated by two coils. The thermal camera measures the temperature of an object before pressing. Data from the thermal camera had from time to time higher values than it should have.

At first, it was found events with higher temperature values (from a thermal camera). This data was checked and analysed. It was not found any pattern or result in what was causing this problem. It was necessary to do an experiment.

5.1.2 Design

The measured object was bent tube (shown in Fig. 16 and Fig 17). The tube was heated by coils, and each end was measured by pyrometer – left pyrometer for the left end (here hereinafter referred to as P_L) and right pyrometer for a right end (here hereinafter referred to as P_R). After the bar went to a mechanical press, where each end was pressed separately but before it was pressed, the temperature was measured (each end separately before pressing). Their temperature was measured by the thermo-camera (T_L – left end, T_R – right end) and our calibrated pyrometer (UP_L – left end, UP_R – right end). Both calibrated pyrometers measured a single point at the end of the bar, but the thermal camera measured the whole captured area (shown in Fig). Also, during measurement, we used different emissivity to see a difference. The whole scheme is shown in Fig. 16.

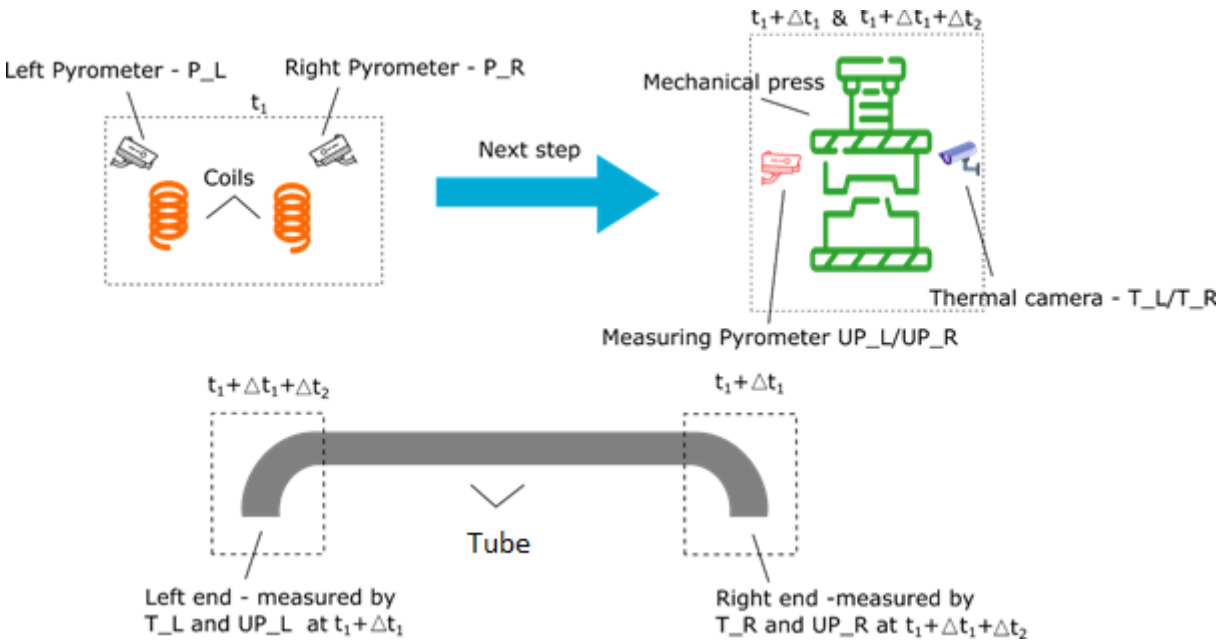

Fig. 16: Scheme of experiment. The time t_1 – Time when the bar is heated at the coil and measured by the pyrometer. The time delay Δt_1 from time t_1 to time when the temperature of the right end of the bar is checked by the thermal camera and measured by our pyrometer, $\Delta t_1 = 5$ sec Δ before pressing. The time delay Δt_2 - from time $(t_1 + \Delta t_1)$ to time when the temperature of the left (second) end of the bar is checked by a thermal camera and measured by our pyrometer; $\Delta t_2 = 11$ sec before pressing.

The measuring position for camera and pyrometer is shown in Fig. 17.

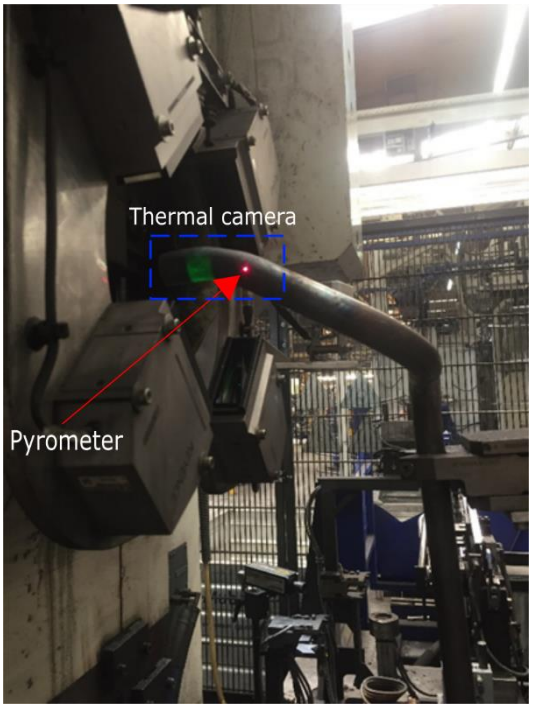

Fig.17: Measuring position fort camera and pyrometer on a bar

5.1.3 Measured data

The measured data are shown in Fig. 18.

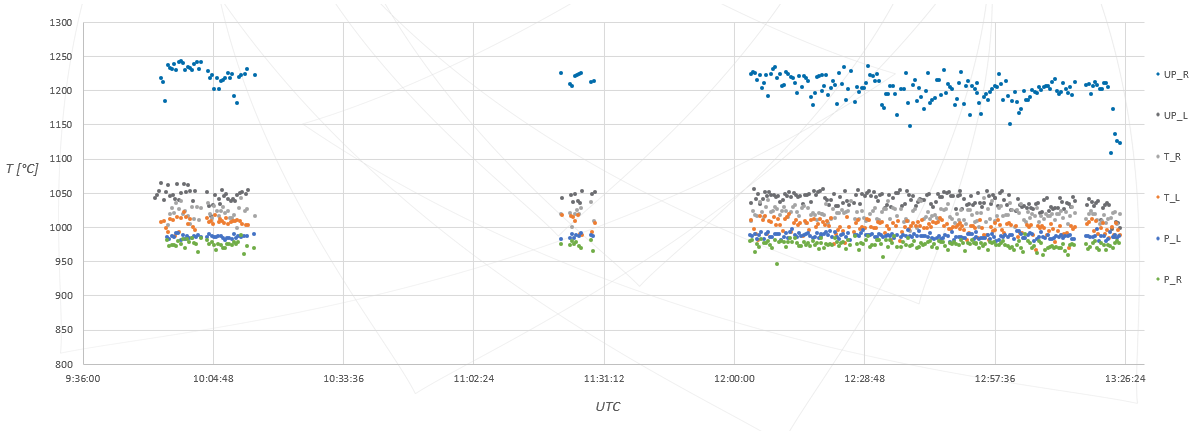

Fig. 18: Measured data from all devices

This measurement was examining the influence of emissivity on measuring devices and temperature analysis. Data can be seen in Fig. 17. Used devices were P_L, P_R, T_R, T_L, UP_L, UP_R. These devices working at conditions that are described in chapter 6.1.2 In measurement are noticeable gaps, technical breaks cause these gaps. During these breaks, the whole process was stopped to setup/repair or align measuring devices. This measurement is divided into six tests, where is every device investigated that correlate with test, and results are described.

5.1.4 Tests

This measurement consists of five tests:

- Emissivity evaluation
- Right end test
- Left end test
- Measurement after heating
- Measurement before press with thermal camera
- Measurement before press with pyrometer

These tests are described and evaluated later in the text.

5.1.5 Influence of emissivity values on the measurement

This test is focused on emissivity dependence on temperature measurement. During this measurement was emissivity changed on UP_L and UP_R during measurement. For this measurement is used the same device but ends are measured at different time.

5.1.5.1 Measured data

The measured data are shown in Fig. 19.

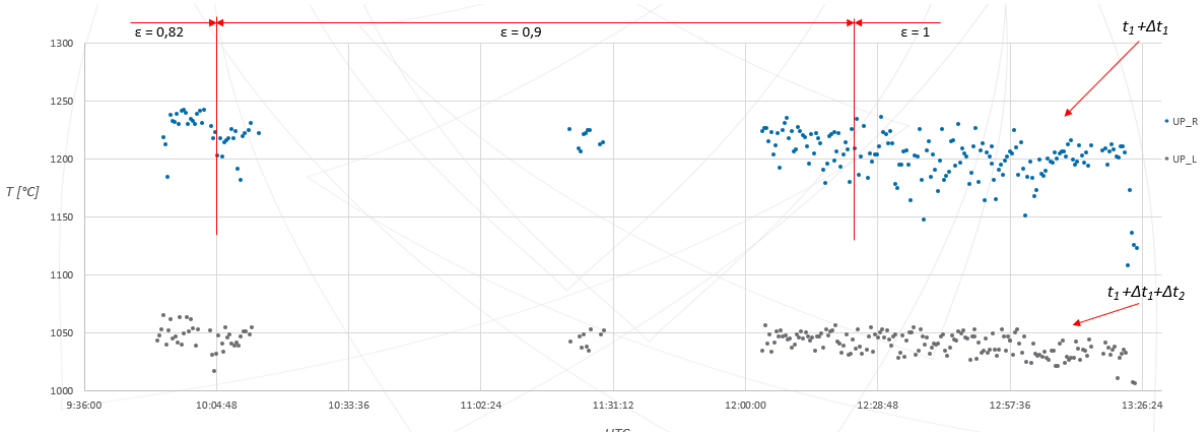

Fig. 19: Measured data from UP_L and UP_R with different emissivity

The emissivity was changed during a measurement. Regions with different emissivity can be seen in Fig.17. From Fig. 17 and Table 1, it is evident that with higher emissivity, the temperature decreases. The statistics can be seen in Table 1.

Statistical parameter	UP_R - 0,82	UP_L - 0,82	UP_R - 0,9	UP_L - 0,9	UP_R – 1	UP_L – 1
Quantity	19	19	147	147	44	44
Expected value [°C]	1230,6	1050,5	1206, 2	1042, 5	1192,261	1027,814
Deviation of expected value [°C]	3,1	2,0	1,4	0,6	3,7	1,90442
Median [°C]	1232,2	1051,0	1208,6	1044,6	1199,8	1030,5
Standard deviation [°C]	13,7	8, 7	17,5	7,8	24,8	12,63249
Minimum [°C]	1184,1	1038,1	1147,4	1016,7	1107,4	985,2
Maximum [°C]	1241,9	1064,3	1235,6	1055,8	1215,9	1043,9
Sum [°C]	23380,5	19960,1	177306,8	153245,4	52459,5	45223,8

Table 1: Statistical parameters for emissivity evaluation

5.1.5.2 Evaluation

The emissivity is important for measurement and should be developed a system for determinate an emissivity value.

5.1.6. Measurement in an operation mode for the right end of the tube

This test is focused on devices that measured the right end of the tube.

5.1.6.1 Measured data

For this experiment were used data from devices that measure the right end of the bar (P_R, T_R, UP_R). These devices were working at conditions that are described in chapter 6.1.2. Data for P_R and T_R are more uniform than for UP_R, and UP_R temperatures are higher than P_R temperatures, can be seen in Fig 18.

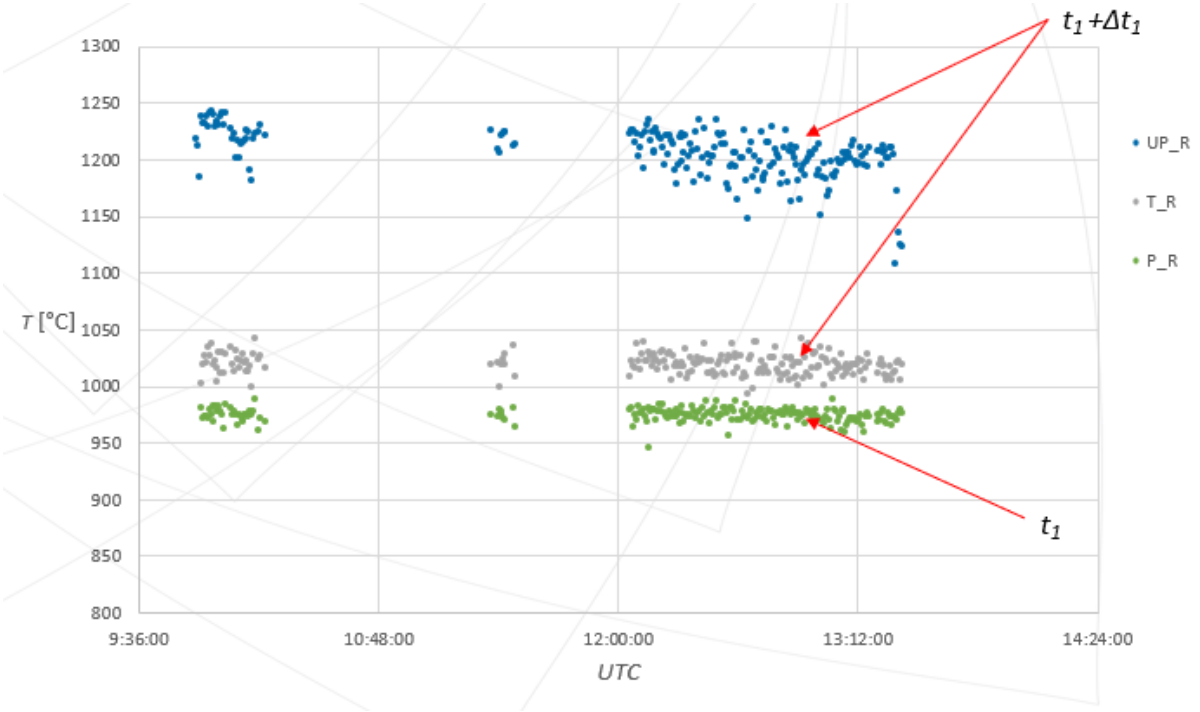

Fig. 20: Measured data from P_R, T_R, UP_R

5.1.6.2 Evaluation

This measurement has not significant nuances for P_R and T_R but for UP_R the measuring is unstable and has a broader spread of data. It is also noticeable that UP_R has higher temperatures than T_R. The T_R measures average temperature from the whole captured area and UP_R measures a single point. Temperatures from T_R are affected by the cooling end that is also measured; this cause that average temperature is lower than other temperature. The statistical parameters are shown in Table 2.

Statistical parameter	P_R	UP_R	T_R
Quantity	210	210	210
Expected value [°C]	974,5	1205, 5	1019,4
Deviation of expected value [°C]	0,4	1,5	0,6
Median [°C]	974,9	1206,8	1019,3
Standard deviation [°C]	5,8	21,3	9,4
Minimum[°C]	945,6	1107,4	993,4
Maximum [°C]	989,2	1241,9	1052,9

Table 2: Statistical parameters for P_R, T_R, UP_R

5.1.7 Measurement in an operation mode for the left end of the tube

This test is focused on devices that measured the left end of the tube. For this measurement was used three different devices (two different pyrometers and thermal camera), where one of pyrometer (P_L) was measured at a different time than pyrometer (UP_L) and a thermal camera (T_L)

5.1.7.1 Measured data

Measured data are shown in Fig. 21

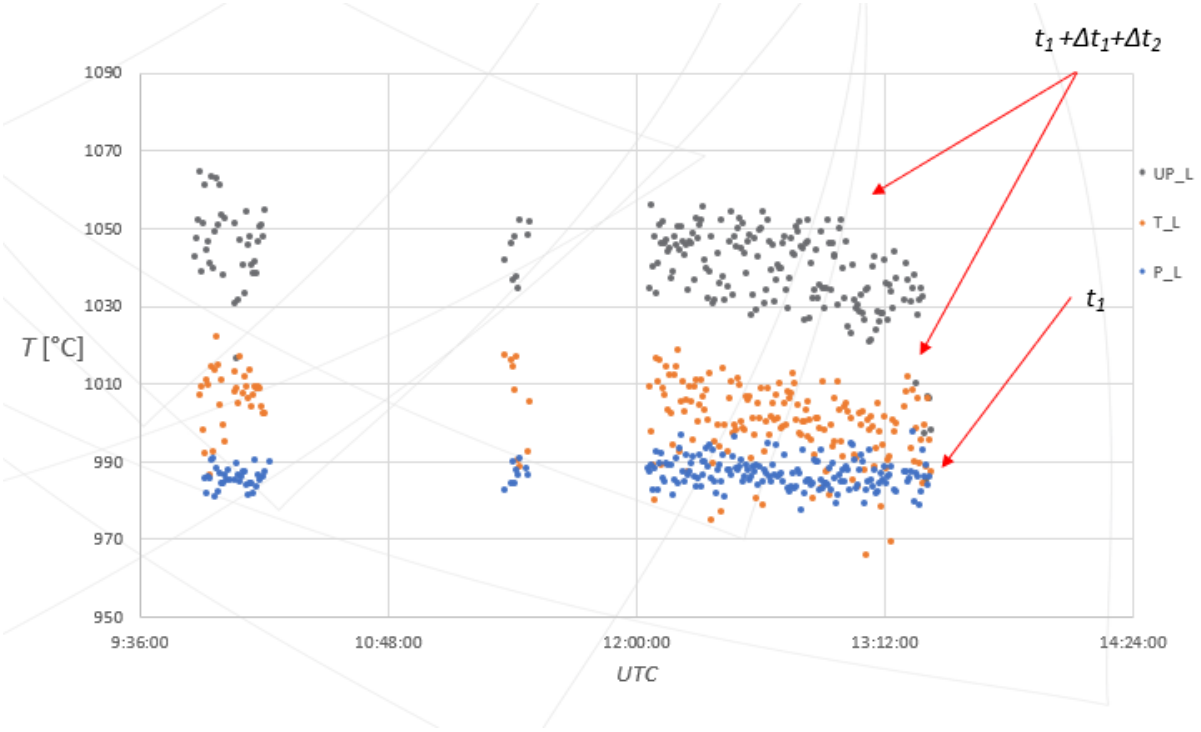

Fig. 21: Measured data for P_L, T_L, UP_L

For this experiment were used data from devices that measure the left end of the bar (P_L, T_L, UP_L). These devices were working at conditions that are described in chapter 6.1.2. The process of for left end is more stable than for right end. The P_L temperatures are lowest, and UP_L are highest.

5.1.7.2 Evaluation

This measurement was more stable than measurement for the right end. The left end had more time for cooling down and stabilise temperature.

Measurements done by T_L are lowest, but measurement done by UP_L are highest, and they measured at the same time. The T_L measures average temperature from the whole field, and UP_L measures a single point on a tube. The end of the tube is a coolest a faster, and when thermal camera measure the whole tube, average are mostly affected by the cooler end. The statistical parameters are shown in Table 3.

Statistical parameter	P_L	T_L	UP_L
Quantity	210	210	210
Expected value [°C]	986,7	1000,9	1040,1
Deviation of expected value [°C]	0,2	0,8	0,8
Median [°C]	986,4	1001,3	1041,6
Standard deviation [°C]	3,5	9,8	11,3
Minimum [°C]	977,6	965,9	985,2
Maximum [°C]	997,6	1022,2	1064,3

Table 3: Statistical parameters for P_L, T_L, P_L

5.1.8 Temperature comparison for both ends after heating

This test focused on pyrometers that measured tube after a heating.

5.1.8.1 Measured data

For this experiment were used only data from P_L and P_R. These devices working at conditions that are described in chapter 6.1.2 Temperatures are different at both ends even if the heating is in the same time.

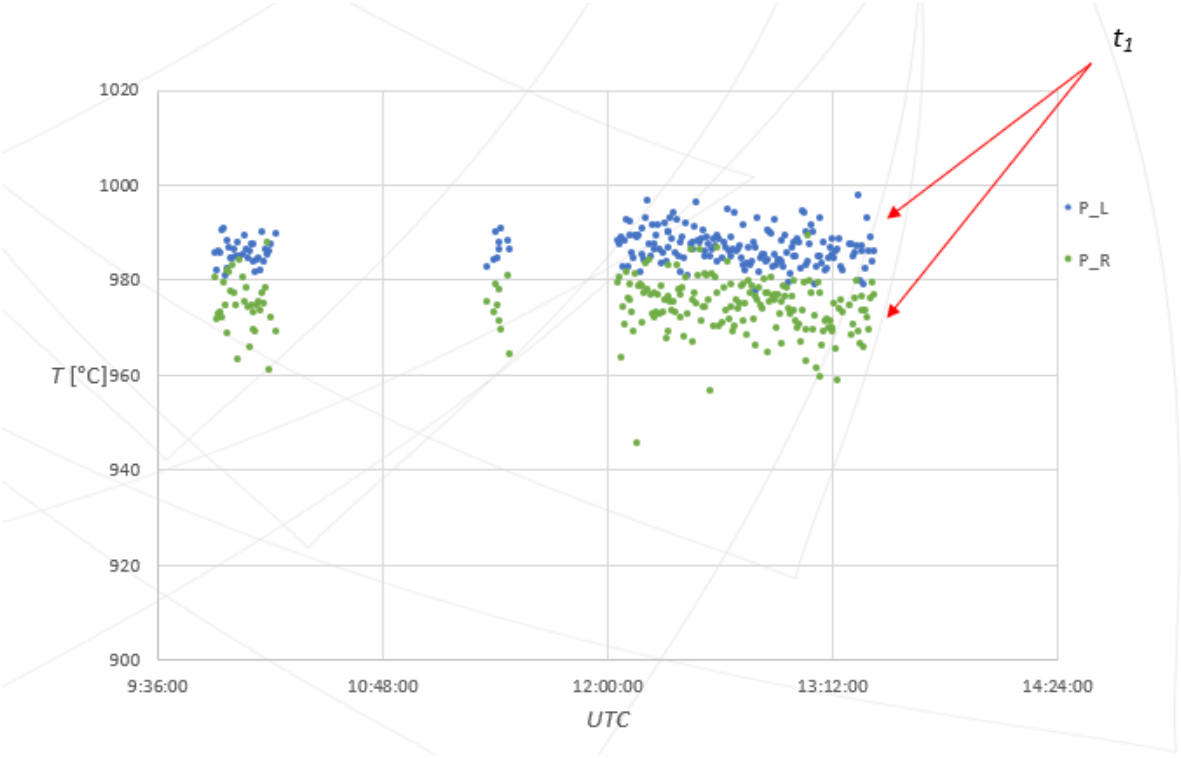

Fig. 22: Measured data for P_L, P_R

5.1.8.2 Evaluation

Temperatures measured by P_L were higher because coils that were heating worked on a different frequency. For the left end, higher frequency is used to minimise temperature loss that is caused by waiting to be pressed. The right end is first to be pressed, and the left end is second. The statistical parameters are shown in Table 4.

Statistical parameter	P_L	P_R
Quantity	210	210
Expected value [°C]	986,7	974,5
Deviation of expected value [°C]	0,2	0,4
Median [°C]	986,4	974, 9
Standard deviation [°C]	3,5	5,
Minimum [°C]	977,6	945,6
Maximum [°C]	997,6	989,2

Table 4: Statistical parameters for UP_L, UP_R

5.1.9 Temperature comparison for both ends before pressing with the pyrometer

This test is focused on pyrometer that measured the tube at the same time as the thermal camera.

5.1.9.1 Measured data

Measured data are shown in Fig. 22

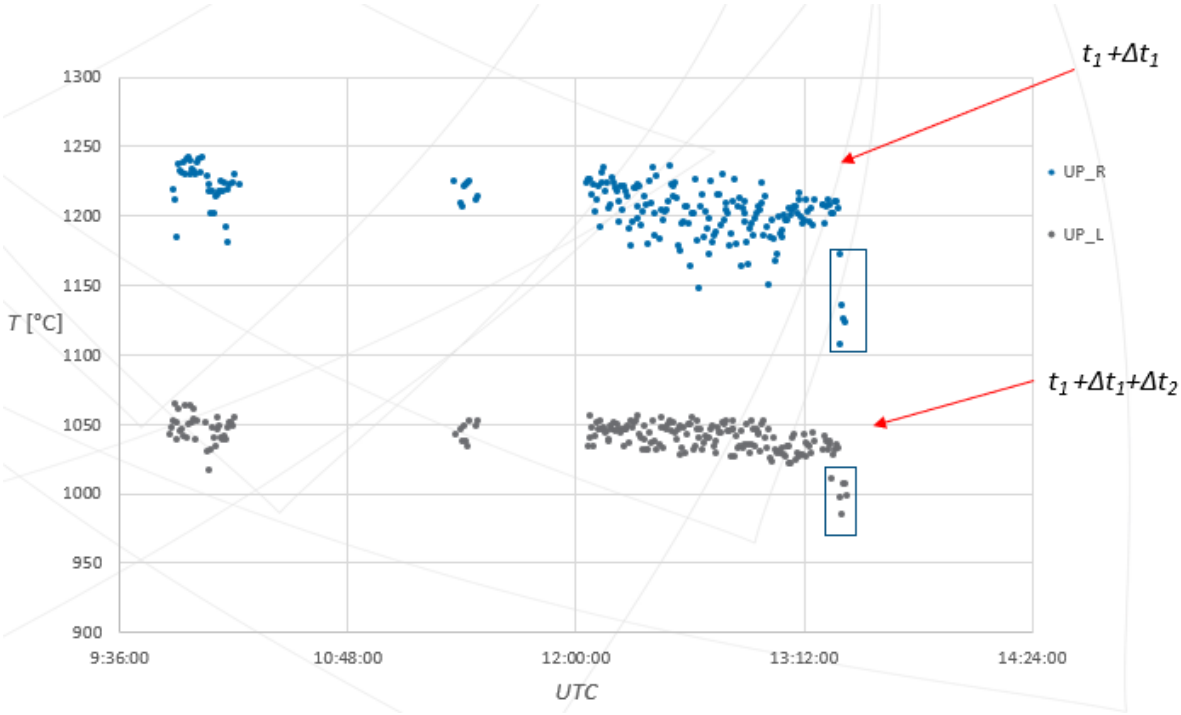

Fig. 23: Measured data for UP_L, UP_R

For this experiment were used only data from UP_L and UP_R. These devices were working at conditions that are described in chapter 6.1.2. The process is more unstable for the right end than the left end. The process of for left end is more stable than of a right end process. ¨

5.1.9.2 Evaluation

UP_R has more unstable temperatures than UP_L. It is caused by cooling and temperature stabilisation. UP_R had less time for stabilisation than UP_R. The data at the end of the graph (highlighted in the figure) is caused by different setting – there was a change of products (temperatures). The statistical parameters are shown in Table 5.

Statistical parameter	UP_L	UP_R
Quantity	210	210
Expected value [°C]	1040,1	1205,5
Deviation of expected value [°C]	0,8	1,5
Median [°C]	1041,6	1206,8
Standard deviation [°C]	11,3	21,3
Minimum [°C]	985,2	1107,4
Maximum [°C]	1064,3	1241,9

Table 5: Statistical parameters for UP_L, UP_R

5.1.10 Temperature comparison for both ends before pressing with the thermal camera

This test is focused on the thermal camera that measured both ends before the tube was pressed.

5.1.10.1 Measured data

The measured data are shown in Fig. 24.

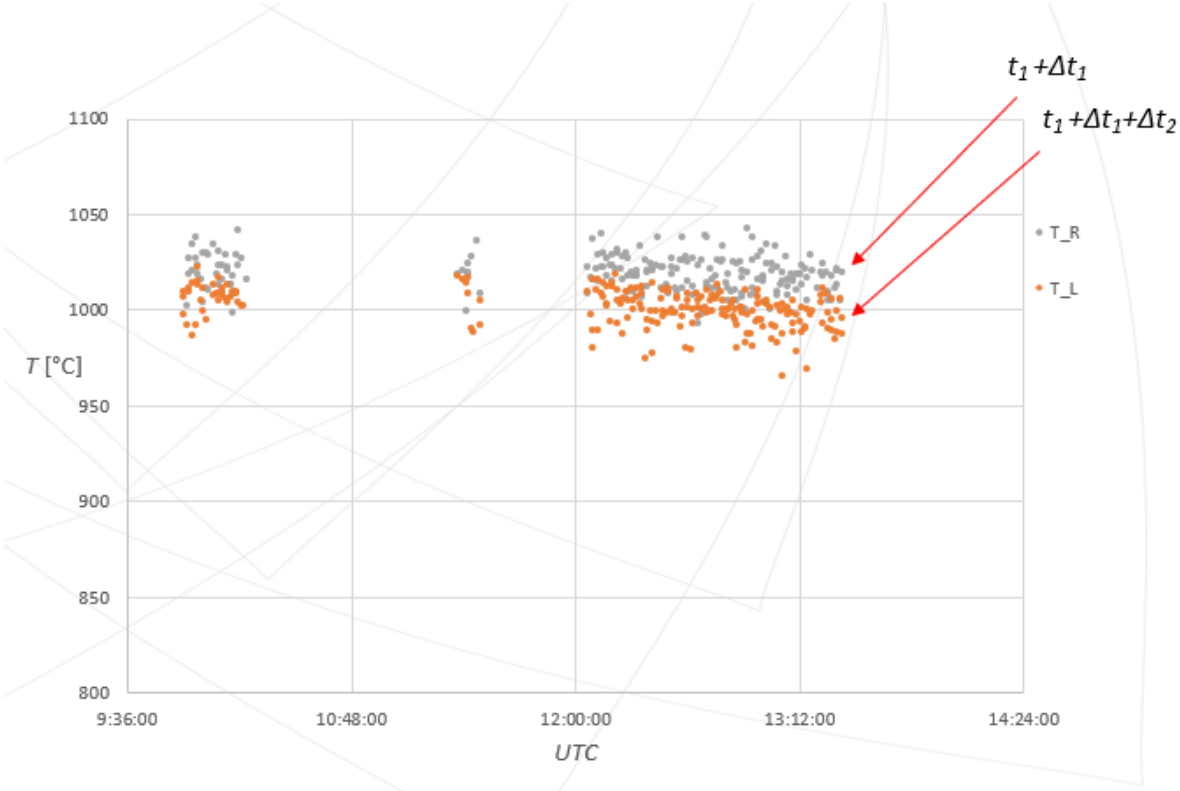

Fig. 24: Measured data for T_L, T_R

For this experiment were used only P_L and P_R. These devices were working at conditions that are described in chapter 6.1.2. Both measurements have a similar standard deviation, but temperatures measured by T_R were higher than other temperatures. It is also noticeable that the data are less uniform than other measured data.

5.1.10.2 Evaluation

The temperatures from the right side are higher because the right side was measured first, and the left side was second. Data are less uniform than from other measurements. This is caused by thermal camera measurement. The thermal camera measures hot surface and makes higher or average temperature on the other side pyrometer always measure the same single point. This makes wide temperature spread. The statistical parameters are shown in Table 6.

Statistical parameter	T_L	T_R
Quantity	210	210
Expected value [°C]	1000,9	1019,4
Deviation of expected value [°C]	0,8	0,6
Median [°C]	1001,3	1019,3
Standard deviation [°C]	9,8	9,408197
Minimum [°C]	965,9	993,4
Maximum [°C]	1022,2	1052,9

Table 6: Statistical parameters for T_L, T_R

5.1.11 Results

5.1.11.1 Influence of emissivity values on the measurement

- The emissivity changes a temperature
- With higher emissivity comes lower temperature
- The emissivity is important for measurement and should be the developed system for determinate an emissivity value

5.1.11.2. Measurement in an operation mode for the right end of the tube

Conditions:

- The same end of the tube (left)
- Different measurement device
- Different or the same measurement time for various devices (See figure description)

Conclusions:

- The process of for left end is more stable than for right end. It is caused by cooling and temperature stabilisation.

5.1.11.2. Measurement in an operation mode for the left end of the tube

Conditions:

- The same end of the tube (left)
- Different measurement device
- Different or the same measurement time for various devices

Conclusions:

- The process of for left end is more stable than for right end. It is caused by cooling and temperature stabilisation.

5.1.11.3 Temperature comparison for both ends after heating

Conditions:

- Different end of the tube (left and right)
- Same measurement device
- Same measurement time for various devices (See figure description)

Conclusions:

- Temperatures are different at both ends even if the heating is in the same time. There can be different frequencies at heating coils (different setup) or calibration constant of measuring devices.

5.1.11.4 Temperature comparison for both ends before pressing with the pyrometer

Conditions:

- Different end of the tube (left and right)
- Same measurement device
- Different or the same measurement time for various devices (See figure description)

Conclusions:

- The process of for right end is more unstable than the left end. The temperature is not stabilized.
- The process of for left end is more stable than of a right end process. It is caused by cooling and temperature stabilisation.
- The data at the end of the graph (highlighted in the figure) is caused by different setting – there was a change of products (temperatures)

5.1.11.5 Temperature comparison for both ends before pressing with the thermal camera

Conditions:

- Different end of the tube (left and right)
- Same measurement device
- Different measurement time for various devices (See figure description)

Conclusions:

- The thermal camera measures hot surface and makes higher or average temperature

5.2 Spectral temperature measurement

5.2.1 Introduction

When optical devices are used for temperature measurements like pyrometer or thermal camera. It is essential to know the emissivity of the measured object. From the previous experiment (chapter 6.1.5) it can be seen changes for different emissivity. That means with precise emissivity value; we get a precise measurement. A significant factor for emissivity is a material surface. For example, polished metal has a lower emissivity than oxidised metal. This behaviour is critical for precise optical temperature measurement.

5.2.2 Design

For measuring it were used two clean object – steel tube and steel rod. To objects were attached thermocouple for reference temperature measurement. The objects were separately heated for, and their spectrums were measured for different temperatures as the heating process was used induction heating. It was necessary to manipulate with the object. When objects were heated, it was placed on a holder, where was spectrometer ready for measurement (the scheme is shown in Fig.25).

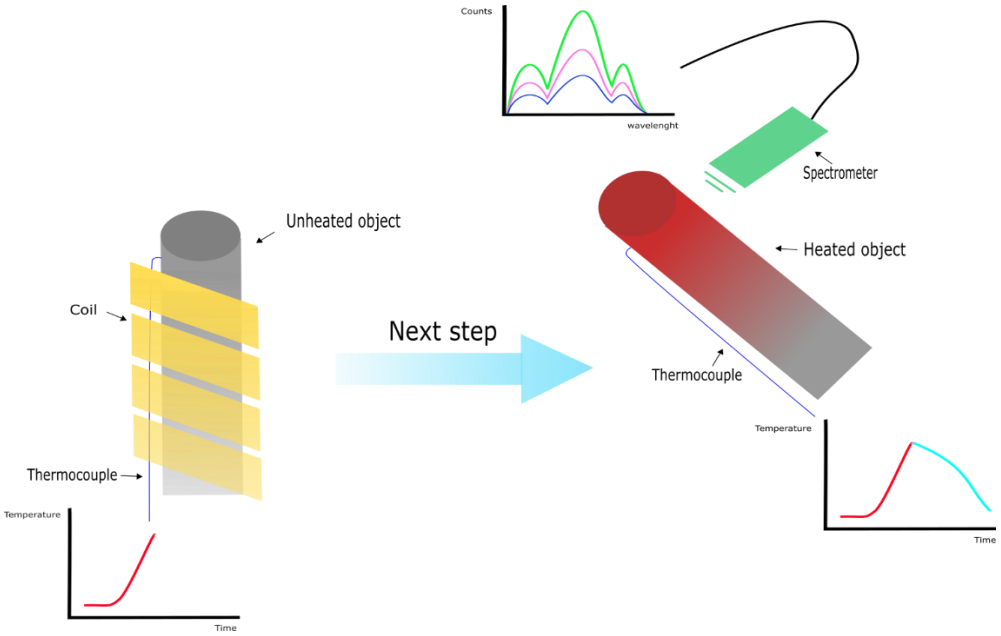

Fig. 25: Scheme of the experiment

After heating, both objects were used for another measurement. From Fig, 26 it is noticeable that rod is changed her structure (same it with tube).

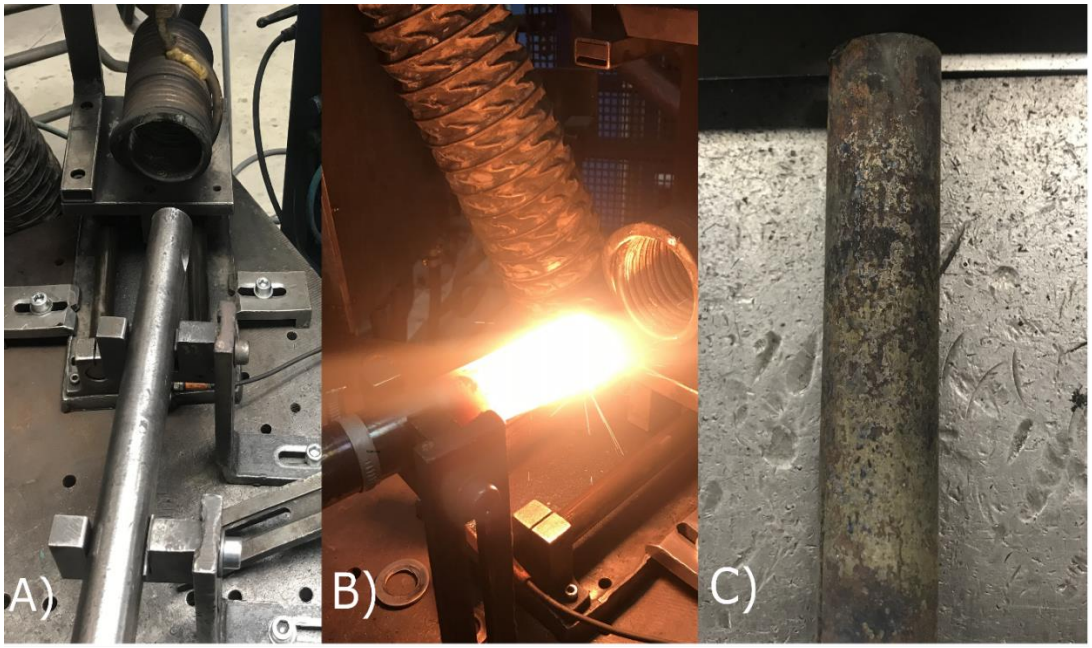

Fig. 26: The testing process: A) Clean rod B) Heated rod D) Used rod

The time course for heating and cooling is shown in Fig.27.

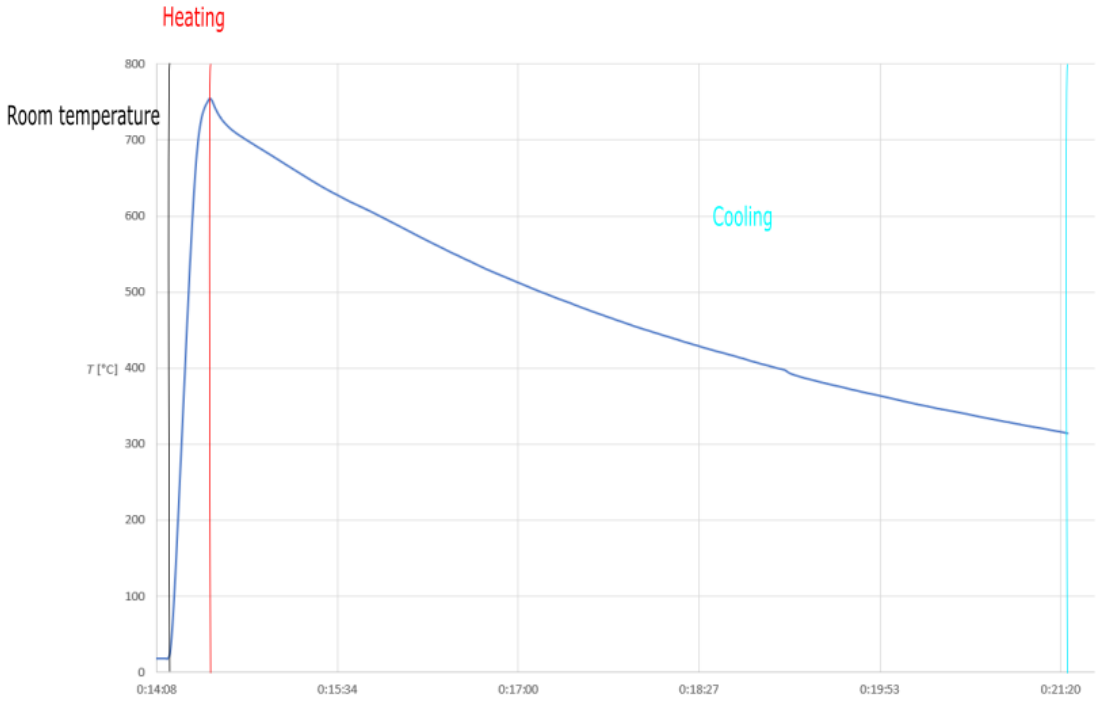

Fig. 27: Graph of heating and cooling with marked areas

5.2.3 Technique of fitting

For the fit, it is important to find y value. The y value is the area under the cooling curve that is limited in the spectrum (shown in Fig. 28).

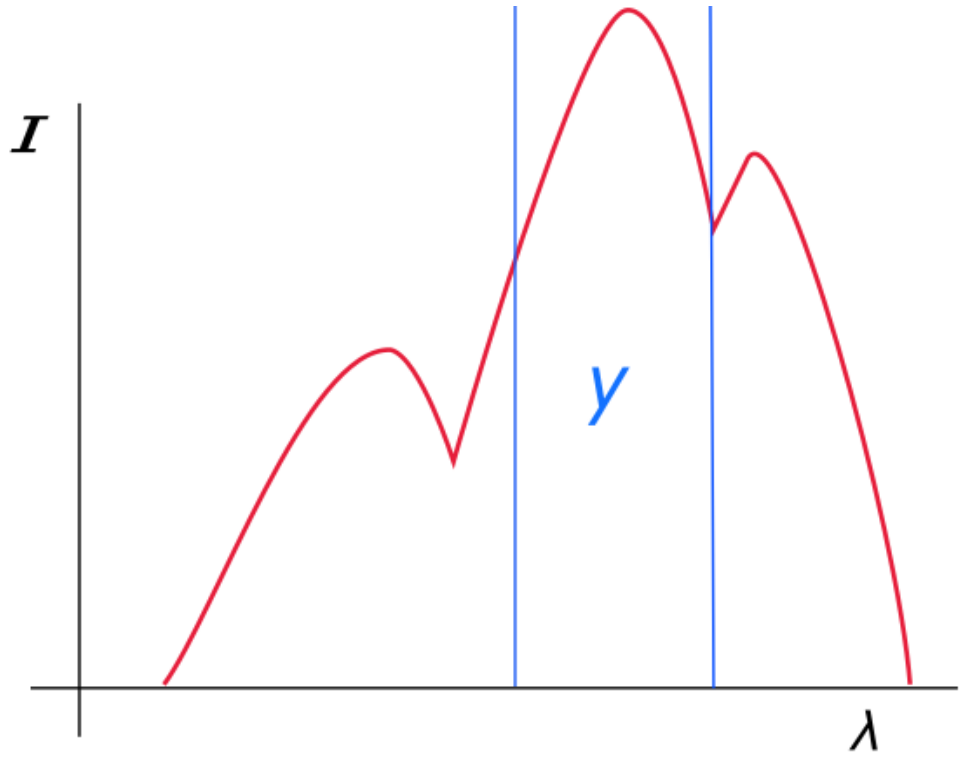

Fig. 28: The meaning of parameter y

For certain temperatures were done curve fitting. Used Fitting curve was:

$$y = aT^4 + b, \tag{49}$$

where a, b are fitting parameters, and T is a temperature. The a parameter affects slope a curve, and b parameter affects shift a curve in y direction (shown in Fig. 29). These properties can be seen in Fig. 28. The surface area of the graph is calculated in certain limits (limits are caused by properties of the spectrometer). The missing part of the intensity is compensated by adding parameter b.

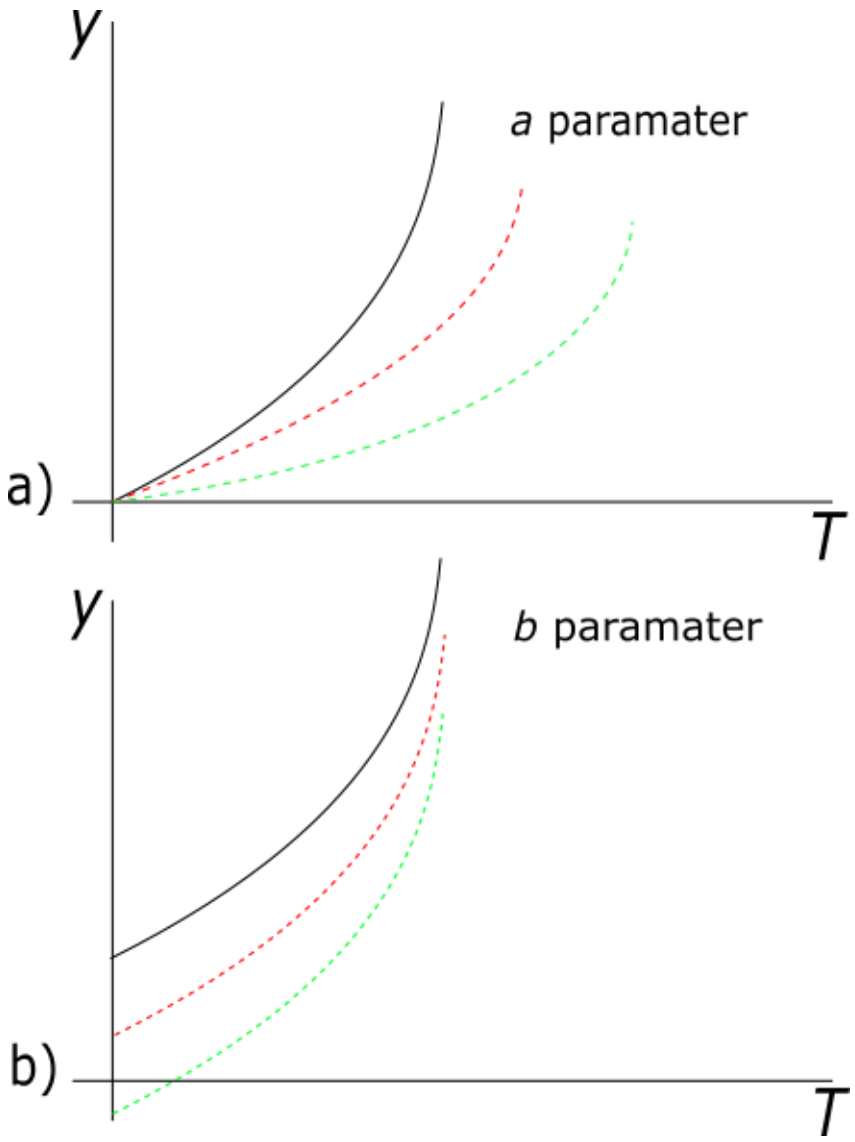

Fig. 29: Properties of a, b parameters.

For analysis is important a parameter because the fitting curve is real Steffan - Boltzman law. The a parameter can be described as:

$$a = \varepsilon k \sigma, \tag{50}$$

where ε is emissivity, k unknown constant and σ is Stefan-Boltzmann constant. The only variable in is emissivity and unknown constant.

Spectrometer is not calibrated on radiation intensity in intensity units. This is compensated by k constant in formula (46) (constant k is unknown). The output intesity is proportional radiation intensity. Comparing a parameter from other fitting gives answer if the emissivity is same or not.

5.2.4 The rod

For this measurement was used the rod as measuring object.

5.2.4.1 Measured data

The measured spectrum for the rod is shown in Fig. 32

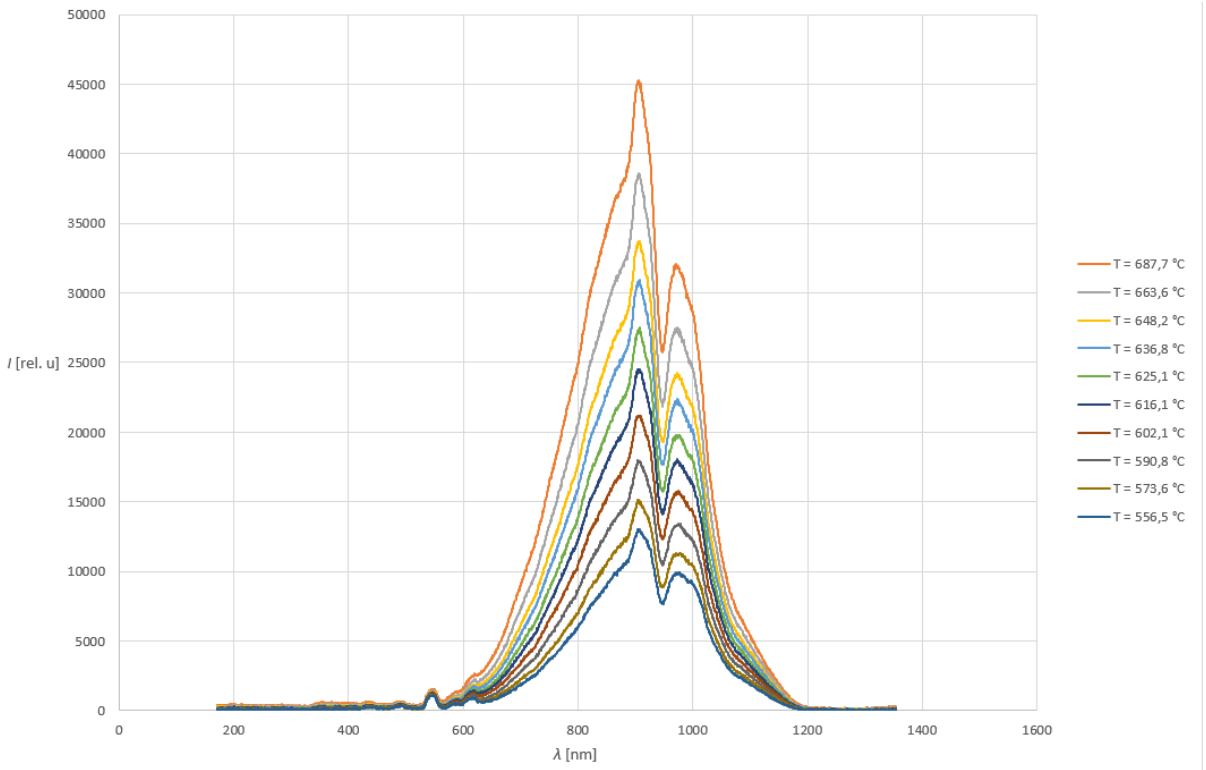

Fig. 30: Measured spectrums for the rod

The temperature course for the rod is shown in Fig. 31.

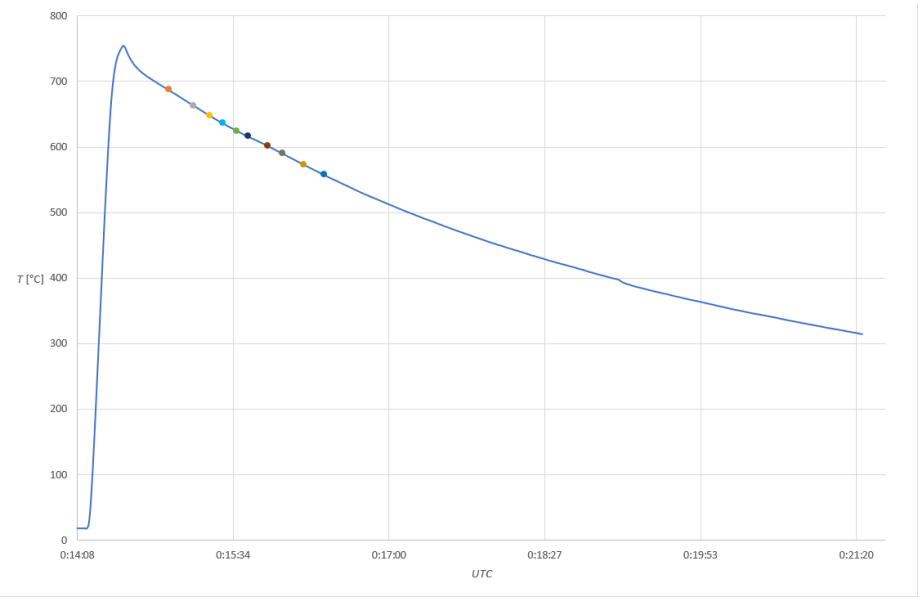

Fig. 32: Temperature course for the rod with temperature spots where was spectrum was taken (each colour belongs to spectrum that is shown in Fig 29)

5.4.2.2 Evaluation

The steel rod was heated for a certain time, and after was moved on a holder. From the point when was rod placed on holder spectrum measurement started. When was spectrum captured specific time was write down. After the measurement, it was necessary to assign certain temperatures with the time that belongs to a spectrum. When the temperature felt down above 500 °C measurement ended. The temperature was falling down pretty quickly. This was common for all our measurements. This is noticeable in Fig. 30.

For rod the fitting parameters curve is:

$$y = 6.34 \cdot 10^{-5}\, T^4 - 3{,}39 \cdot 10^6 \tag{51}$$

The fitting curve can be seen in Fig 31.

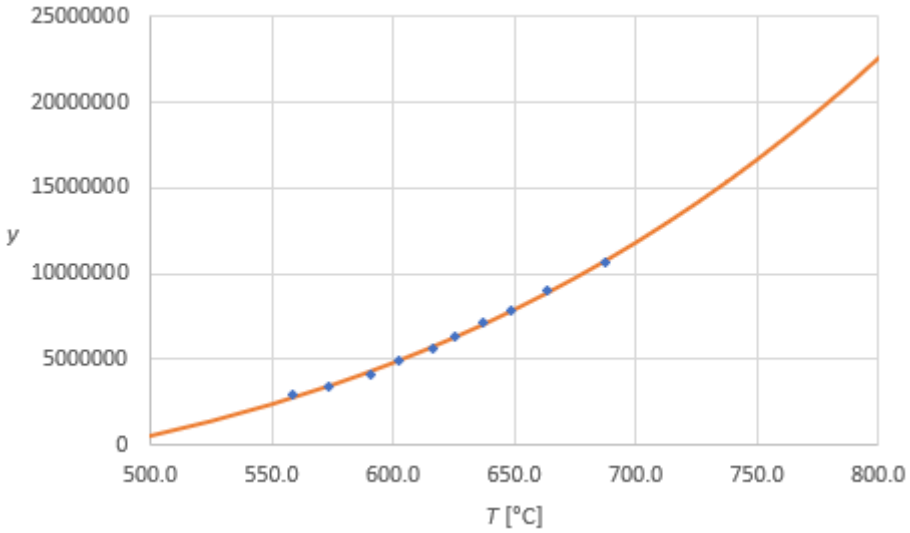

Fig. 31: Fitting curve for the rod

5.2.5 The regular tube

For this measurement was used the regular tube

5.2.5.1 Measured data

The measured spectrum for the regular tube is shown in Fig. 32

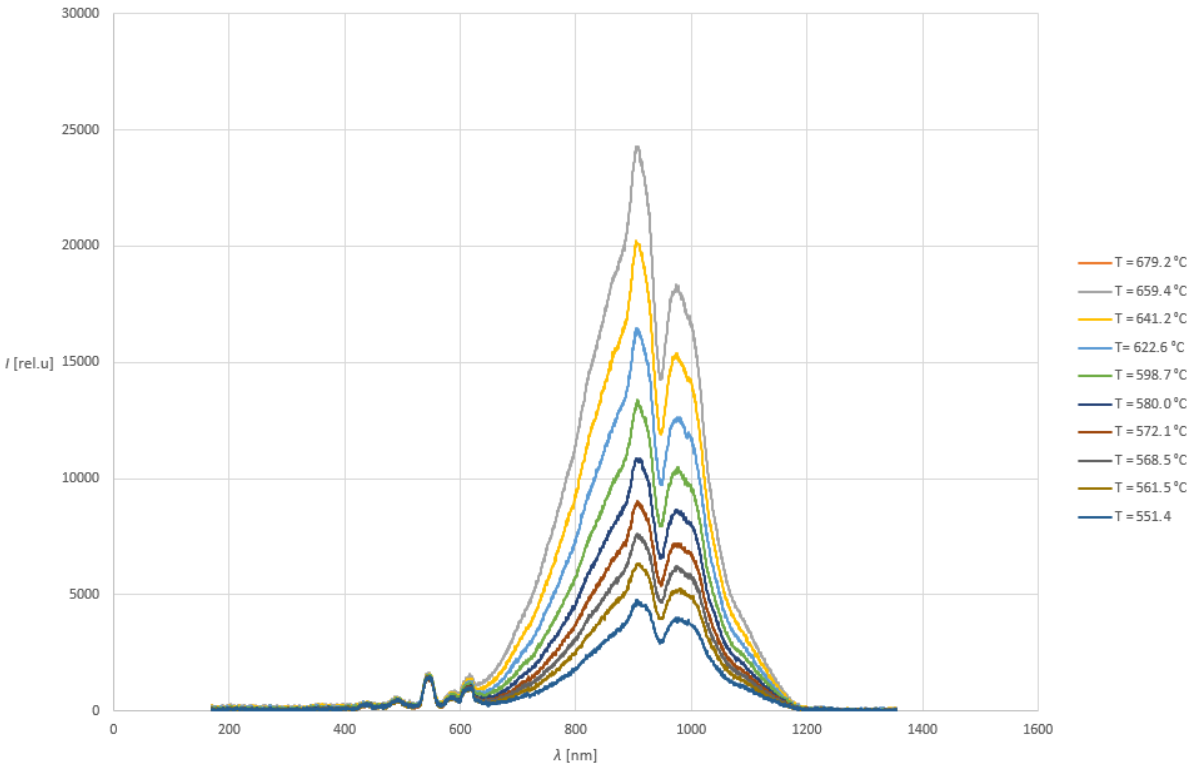

Fig. 32: Measured spectrums for the regular tube

The temperature course for the regular tube is shown in Fig. 36.

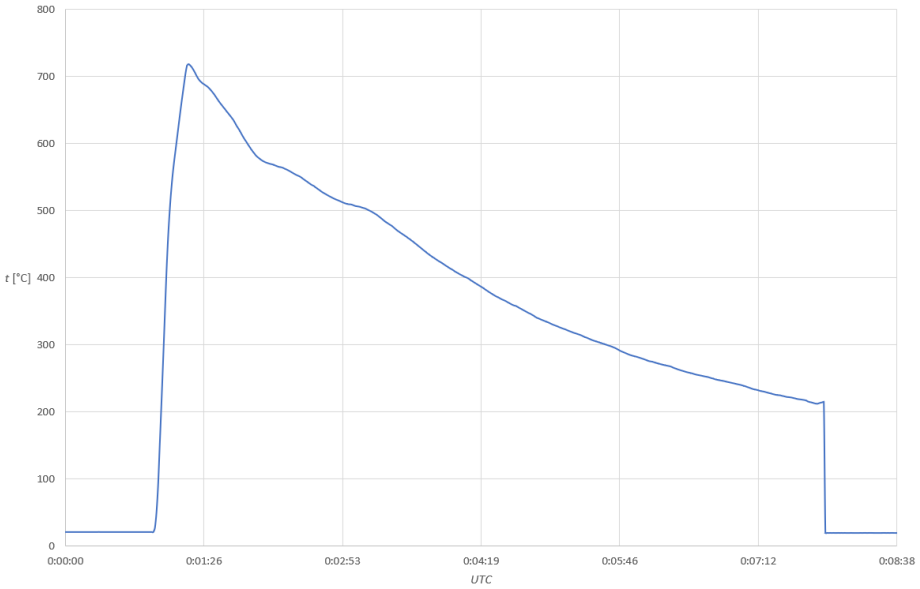

Fig. 33: Temperature course for the regular tube

The measurement and data evaluation were done the same as previous measurement, but it was used a different object – steel tube.

5.2.5.2 Evaluation

The main difference between tube and rod is that tube is hollow—the amount of This effect of radiation that is emitted. The rod emitted a large amount of radiation than a tube. That means the emissivity is different for rod and tube. This also confirms Fig where was done fitting. The fitting curve for the tube is: (52)

$$y = 3.66 \cdot 10^{-5} T^4 - 2{,}41 \cdot 10^6.$$

The fitting curve for the tube can be seen in Fig 34.

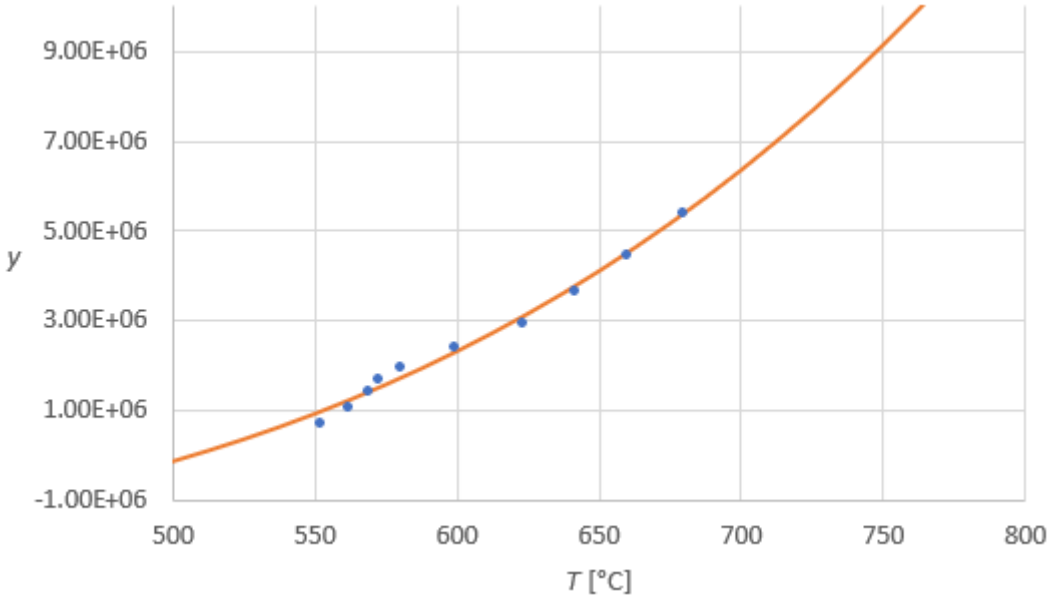

Fig.34: Fitting curve for the regular tube

If we compare fitting parameters for tube and rod, there is a difference in both fitting parameters. The ratio of a parameters for the tube and the rod is 57.7%. This result is important because it says tube and rod have different emissivity. In Stefan-Boltzman law (described in the chapter), the temperature is dependent on the emissivity of the measured object. That means the thermal measurement is different for those two objects, and it is crucial to know the value of emissivity for measured objects separately.

5.2.6 The used tube

For this measurement was used the used tube

5.2.6.1 Measured data

The measured spectrum for the used tube is shown in Fig. 35

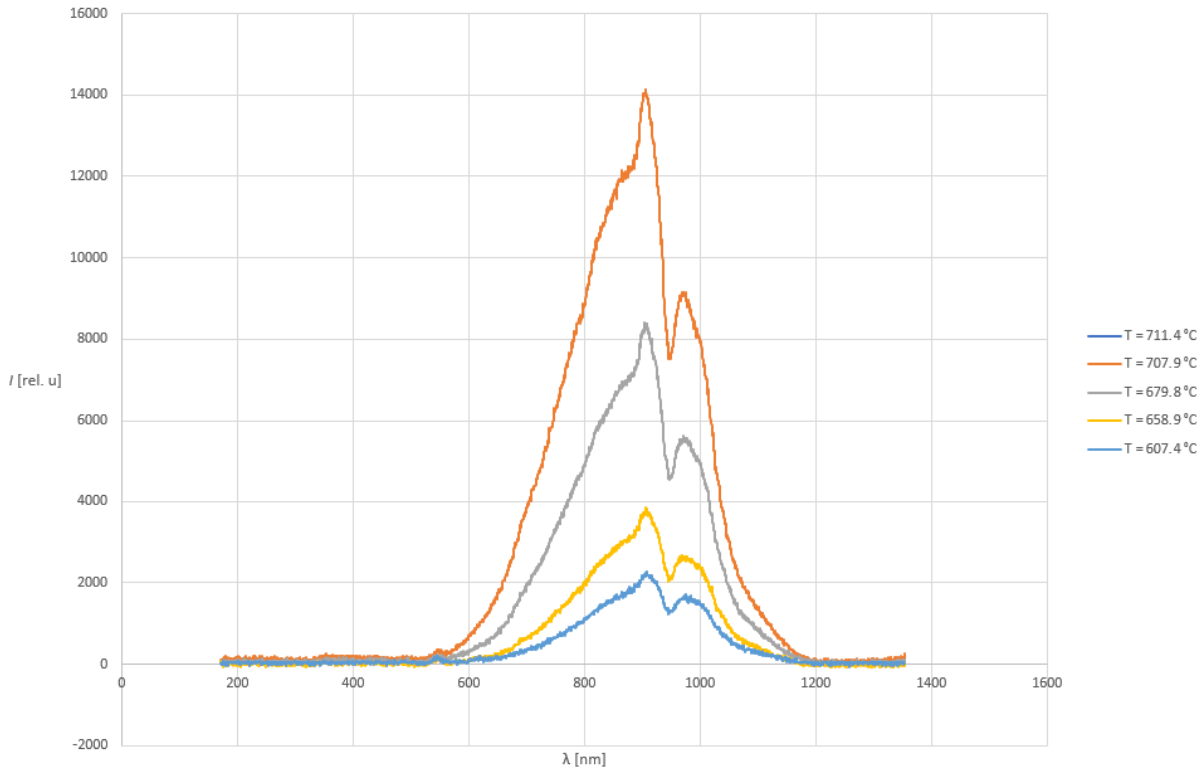

Fig. 35: Measured spectrums for the used tube

The temperature course for the used tube is shown in Fig. 36.

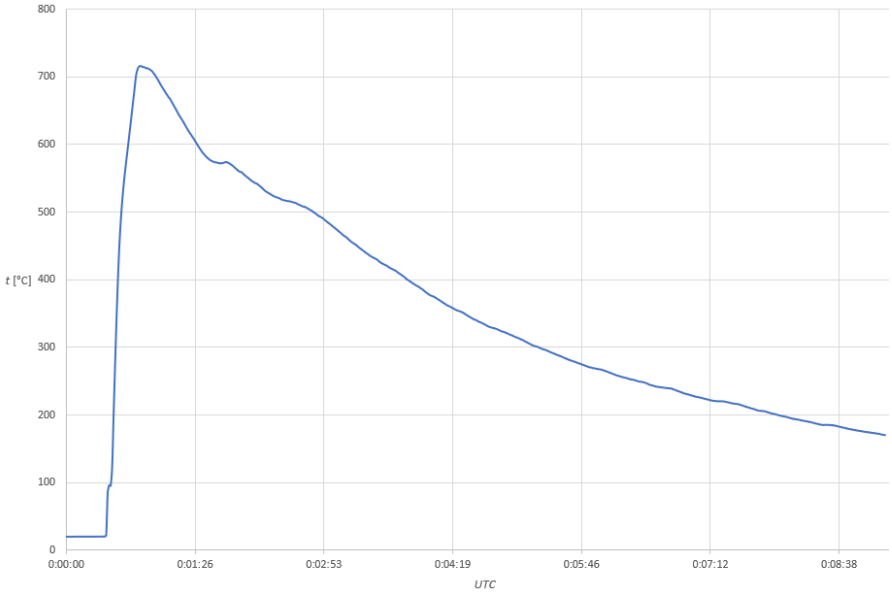

Fig.36: Temperature course for the used tube

The measurement and data evaluation were done the same as previous measurement, but it was used different object – already used steel tube. The tube changed its surface (see Fig. 24)

5.2.6.2 Evaluation

The fitting curve for the tube is:

$$y = 3.48 \cdot 10^{-5} T^4 - 4.93 \cdot 10^6. \tag{53}$$

Fitting curve for the used tube can be seen in Fig. 35.

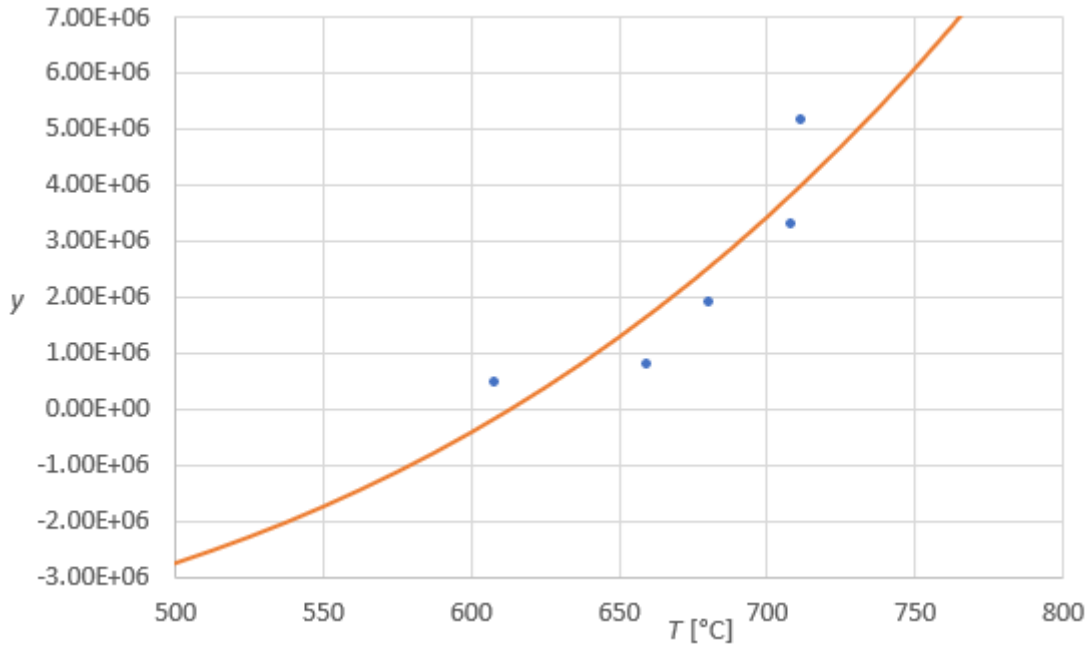

Fig. 37: Fitting curve for the used tube

The ratio of a paramaters for the tube and used tube is 95%. The result from the fitting curve is very similar to the regular tube. The emissivity value is very similar, and the difference does not affect the emissivity. The parameter b is different for tube and used tube because the geometry of the experiment could be different, or exposure time was different etc.

5.2.7 Results

- The tubes and rod have different emissivity. It is crucial to set a specific value for tube and rod
- The regular tube and used tube have very similar emissivity. The emissivity value is very similar, and the difference does not affect the emissivity.
- The measured temperatures for each object can be seen in Fig. 38.

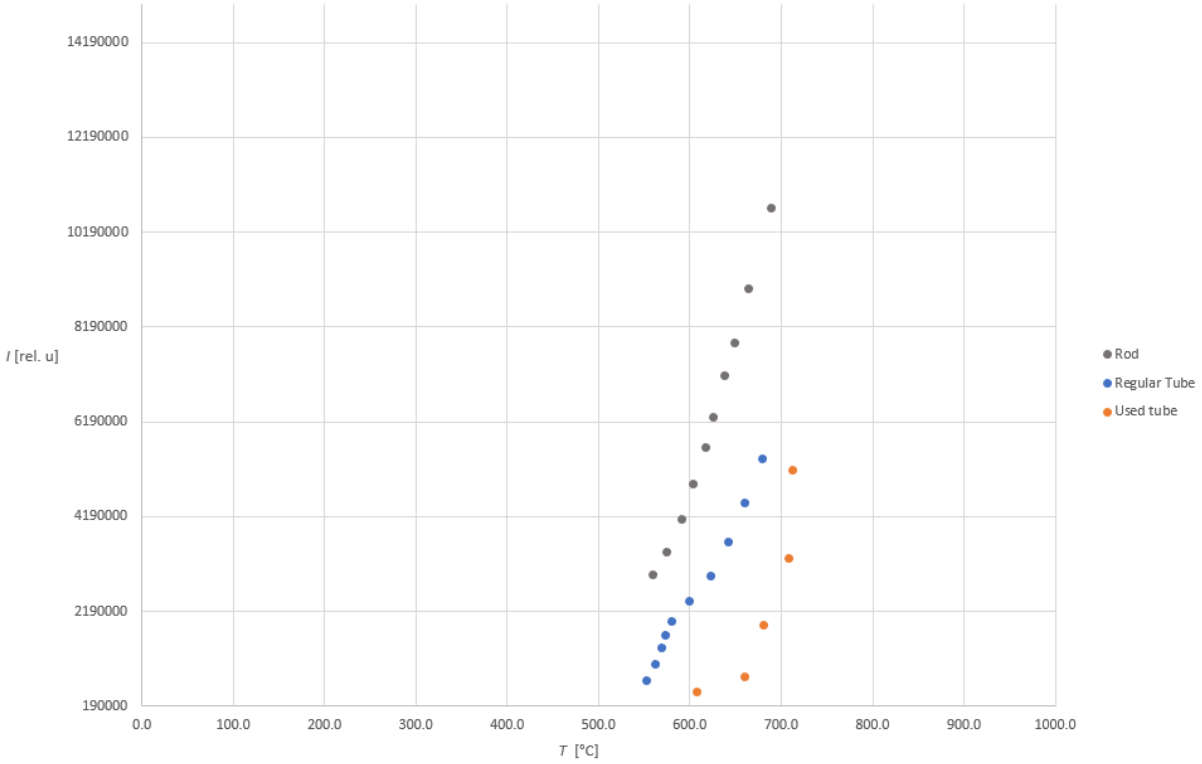

Fig. 38: Measured temperatures for each object

- The fitting curves can be seen in Fig. 39.

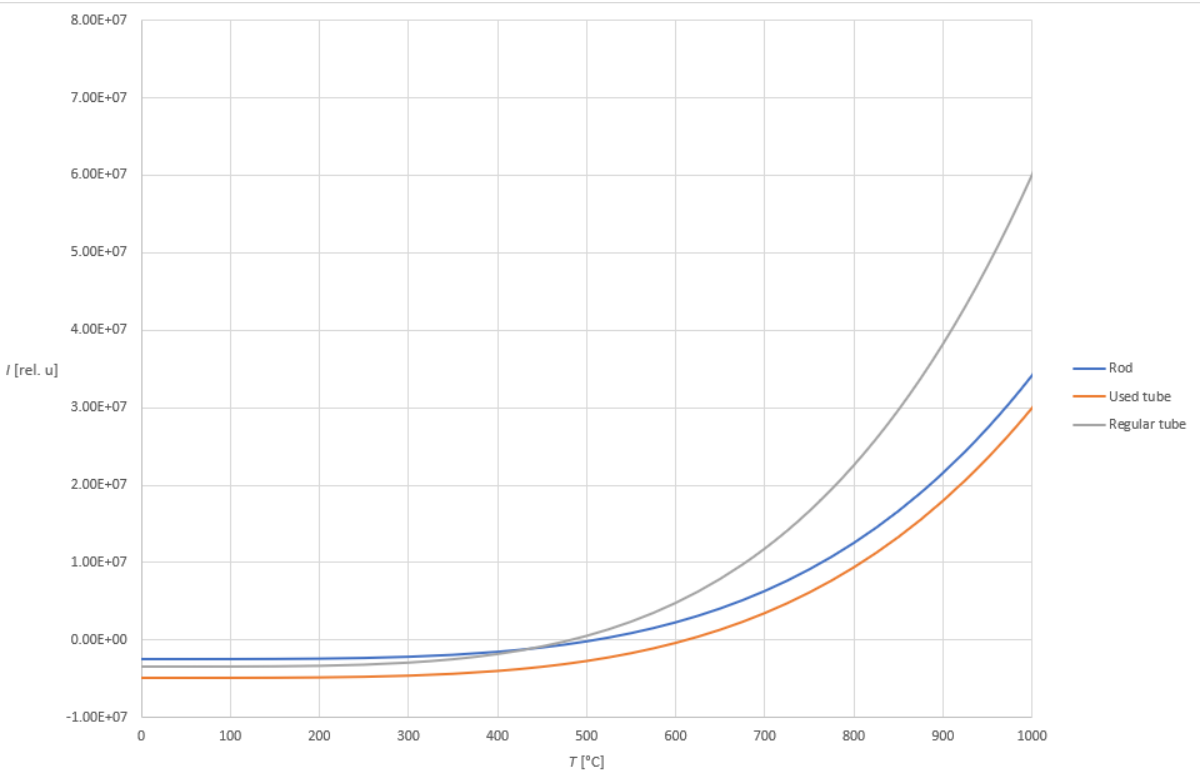

- **Fig. 39:** Fitting curves for each object

- The fitting curves without parameter b can be seen in Fig. 40

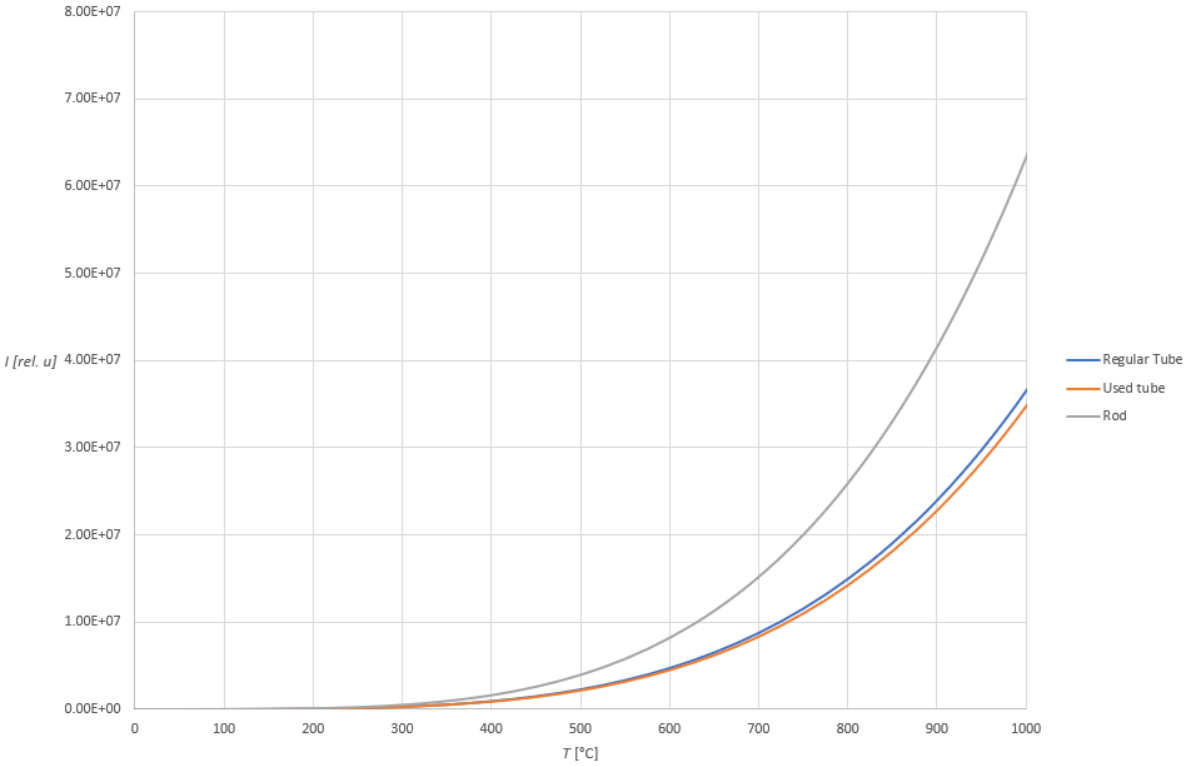

Fig. 40: Fitting curves for each object without parameter b

- There should be a future experiment that determines emissivity and test different sizes of tube and rod is there any difference.

6 Conclusion

This work is focused on temperature measurement in the industrial environment. For the measurement, it was used non-contact, and contact devices as non-contact devices were used pyrometers, thermal camera and spectrometer and as contact was used thermocouples.

At first, it was important to learn about measuring setup and data acquisition and learn about the environment. This included learning about used measuring devices, setups and limits. This task was exciting because it was different from what I have experienced before. Mostly the limitation of the measurement. For example, if the experiment is done under laboratory condition, it is hard to demonstrate outside the lab. To make it possible you need a rethink and redesign the experiment for that environment.

After all this, there was time to get into the depth of the problem. Before I could handle experiments, I had to learn about the process and industrial environment.

This work is divided into two main experimental parts. First, part was focused on testing measuring devices and their behaviour and the second part was focused on how emissivity affects the measurements.

The first part was investigating the behaviour of four non-contact measuring devices in a industrial process. The process consisted of heating, pressing a steel tube. The devices were two pyrometers thermal camera and third pyrometer. The two pyrometers were measuring the heating. The thermal camera and third pyrometer were measuring the pressing. For the third pyrometer, the emissivity setting was changed during a measurement. It was obtained data with three different emissivity values. This was proof the emissivity affects the measurement. From all used devices, it was obtained a data, and for all these data was done comparison and statistics. This helped me more understand a process but also popped up a few questions about products and how the system works.

The second part was about emissivity behaviour for different objects. The objects were clean rod, clean tube and used tube (different surface thanks to heating). The fitting parameters are similar for clean tube and used tube, that means the emissivity is similar for these two objects However, there was a big difference between fitting parameters for tube and rod, that means the emissivity for both objects are different, and there should be a specific measurement for evaluating emissivity. The futures plan is to get a grant from GACR (Czech Science Foundation) for obtaining better equipment as spectrometer and blackbody to make precise measurement and get these values. For future measurement, it will be essential to make the whole measuring automatic to minimise humans' errors.

There was only highlighted two main experiments, but there were other experiments or some data analysis. The experiments ended as failure and data analysis was mostly done for personal interested to understand the problem indeed.

List of the used sources

[1] GUPTA, Shashikant. *Blackbody radiation* [online]. Indian Institue of Science, Banglore, 2003 [cit. 2020-02-16]. Dostupné z: http://www.iucaa.in/ ~dipankar/ph217/contrib/blackbody.pdf

[2] USAMENTIAGA, Rubén, Pablo VENEGAS, Jon GUEREDIAGA, Laura VEGA, Julio MOLLEDA a Francisco BULNES. Infrared Thermography for Temperature Measurement and Non-Destructive Testing. Sensors [online]. 2014, **14**(7), 12305-12348 [cit. 2020-02-16]. DOI: 10.3390/s140712305. ISSN 1424-8220. Dostupné z: http://www.mdpi.com/1424-8220/14/7/12305

[3] OBDRŽÁLEK, Jan. Úvod do termodynamiky, molekulové a statistické fyziky. Praha: Matfyzpress, 2015. ISBN 9788073782870.

[4] JOHNSON, Claes. Blackbody. In: *Claes Johnson on Mathematics and Science* [online]. [cit. 2020-04-01]. Dostupné z: http://claesjohnson.blogspot.com/2011/11/blackbody-as-bottle-with-peephole.html

[5] HANSSEN, Leonard, Simon G. KAPLAN a Raju V. DATLA. *Infrared Optical Properties of Materials* [online]. NIST, 2015 [cit. 2020-05-20]. DOI: 10.4236. Dostupné z: https://dx.doi.org/10.4236/wet.2014.52004

[6] HAJKO, Vladimír a Juraj Daniel SZABÓ. *Základy fyziky*. 2. doplněné vydání. Bratislava: Veda, 1983.

[7] Two-dimensional plot of the spectrum of a blackbody with different temperatures. In: *John A. Dutton e-Education Institute* [online]. [cit. 2020-04-01].

[8] RIEDL, Max J. *Optical design fundamentals for infrared systems*. 2nd ed. Bellingham, Wash.: SPIE Press, 2001. ISBN 9780819440518.

[9] The intensity of blackbody radiation versus the wavelength of the emitted radiation. In: *Openstax* [online]. [cit. 2020-04-01]. Dostupné z: https://openstax.org/books /university-physics-volume-3/pages/6-1-blackbody-radiation

[10] CHUNG, Deborah D. L. *Carbon composites: composites with carbon fibers, nanofibers, and nanotubes*. Second edition. Boston: Elsevier/BH, Butterworth-Heinemann is an imprint of Elsevier, [2017]. ISBN 978-0-12-804459-9.

[11] MEOLA, Carosena, Simone BOCCARDI a Giovanni Maria CARLOMAGNO. *Infrared Thermography in the Evaluation of Aerospace Composite Materials: Infrared Thermography to Composites*. Woodhead Publishing, 2015. ISBN 978-1-78242-171-9.

[12] BITYUKOV, V. K., V. I. NEFEDOV a D. S. SIMACHKOV. NON-CONTACT METHOD OF MEASURING SURFACE TEMPERATURE. *Russian Technological Journal* [online]. 2019, **7**(2), 5-17 [cit. 2020-05-12]. DOI: 10.32362/2500-316X-2019-7-2-5-17. ISSN 2500-316X. Dostupné z: https://www.rtj-mirea.ru/jour/article/view/144

[13] PRESTON-THOMAS, H. The International Temperature Scale of 1990. In: *Bureau International des Poids et Mesures* [online]. BIPM, 1989 [cit. 2020-03-28]. Dostupné z: https://link.springer.com/content/pdf/bbm%3A978-1-4419-8282-7%2F1.pdf

[14] On the implications ofchanging the definition of the base unit kelvin: Report to the CIPM 2007. In: *Bureau International des Poids et Mesures* [online]. 2007 [cit. 2020-03-28]. Dostupné z: https://www.bipm.org/utils/common/

[15] pdf/CC/CCT/CCT_Report_on_Redefinition.pdf

[16] WANG, S, Juming TANG a F YOUNCE. *Temperature Measurement* [online]. Washington State University, Pullman, Washington, U.S.A. [cit. 2020-02-16]. Dostupné z: https://pdfs.semanticscholar.org/b050

[17] /a481f5a26ad67b84d162ca9135239b7709d3.pdf

[18] Senzor - teploty PT1000-550. In: *Rasel* [online]. [cit. 2020-04-01]. Dostupné z: https://www.rasel.cz/senzor-teploty-pt1000-550-p20543/

[19] KIM, T., T. J. LU a S. J. SONG. *Application of Thermo-Fluidic Measurement Techniques: Chapter 1 - Experimentation in Aerodynamics and Heat Transfer,*. 2016, 1-12. DOI: https://doi.org/10.1016/B978-0-12-809731-1.00001-0. ISBN ISBN 9780128097311. Dostupné také z: http://www.sciencedirect.com/science/article/pii/B9780128097311000010
[20] LACHISH, Uri. *Thermoelectric Effect Peltier Seebeck and Thomson* [online]. [cit. 2020-02-16]. DOI: 10.13140/EG.2.1.2722.3443. Dostupné z: http://urila.tripod.com/Thermoelectric.pdf
[21] *NORME INTERNATIONALE: Couples thermoélectriques*. IEC 584-1. 1995.
[22] HEDDLE, T. *Calculations in Fundamental Physics: Volume II: Electricity and Magnetism*. Elsevier Science, 2013. ISBN 9781483137919.
[23] WU, Joseph. *A Basic Guide to Thermocouple Measurements* [online]. 2018 [cit. 2020-05-21]. Dostupné z: http://www.ti.com/lit/an/sbaa274/sbaa274.pdf?&ts=1590085329757
[24] ORLOV, Igor Ya., Igor A. NIKIFOROV a Alexander V. AFANASJEV. Wireless Infrared Pyrometer with Fiber Optic: Construction and Processing Algorithms. Wireless Engineering and Technology [online]. 2014, 05(02), 25-33 [cit. 2020-02-16]. DOI: 10.4236/wet.2014.52004. ISSN 2152-2294. Dostupné z: http://www.scirp.org/journal/doi.aspx?DOI=10.4236/wet.2014.52004
[25] FELICE, Ralph A. *Pyrometry for Liquid Metals* [online]. 2008 [cit. 2020-02-16]. Dostupné z: http://citeseerx.ist.psu.edu/viewdoc/
[26] download?doi=10.1.1.550.2441&rep=rep1&type=pdf
[27] VAVŘIČKA, Roman. *Bezkontaktní způsoby měření teploty*. Praha: Společnost pro techniku prostředí, 2013. Sešit projektanta - pracovní podklady. ISBN 9788002025153.
[28] IMPAC INFRARED GMBH, Collective of author. *Pyrometer-Handbook* [online]. IMPAC Infrared, GmbH, Krifteler Str. 3260326, Frankfurt am Main Germany [cit. 2020-02-16]. Dostupné z: http://www.irndt.com.cn/html/upfile/2018/10/20181024214754_615.pdf
[29] SOVA, Jan a Karel KADLEC. *Termokamery a pyrometry – princip měření, vlastnosti a využití* [online]. In: . 2014 [cit. 2020-02-16]. Dostupné z: http://www.allforpower.cz/UserFiles/
[30] file/termokamery_1.pdf
[31] BATTALWAR, Pooja, Janhvi GOKHALE a Utkarsha BANSOD. Infrared Thermography and IR Camera. *International Journal of Research In Science & Engineering* [online]. **1**(3) [cit. 2020-02-16].
[32] RAI, Mritunjay. Thermal imaging system and its real time applications: a survey. In: *Journal of Engineering Technology* [online]. 2018 [cit. 2020-02-16]. Dostupné z: https://www.researchgate.net/publication/325685880_Thermal_imaging_system_and_its_real_time_applications_a_survey
[33] *Renewable & sustainable energy reviews*. Amsterdam: Elsevier. ISSN 1364-0321.
[34] MICRO-EPSILON. *Operating Instructions: thermo IMAGER TIM* [online]. In:. MICRO-EPSILON MESSTECHNIK GmbH & Co. KG Königbacher Strasse 15 [cit. 2020-02-16]. Dostupné z: https://www.micro-epsilon.com/download/manuals/man--thermoIMAGER-TIM--en.pdf
[35] Univerzální infračervené kamery. In: *MicroEpsilon* [online]. [cit. 2020-05-12]. Dostupné z: https://www.micro-epsilon.cz/temperature-sensors/thermoIMAGER/universal-thermal-imagers/

[36] *Sensortherm Metis MS09 / MI16 / MI18: Pyrometer in the near infrared for temperature measurements on metals* [online]. In: . [cit. 2020-05-12]. Dostupné z: http://www.jytech.com/information/pdf/ST/Sensortherm-Datasheet_Metis_MS09_MI16_MI18.pdf

[37] Pyrometer Series Metis. In: *Sensortherm* [online]. [cit. 2020-05-12]. Dostupné z: https://www.sensortherm.de/en/pyrometer-series-metis

[38] *PhoenixTM HTS02 Systems: For heat treatment processes above 800°C* [online]. [cit. 2020-05-12]. Dostupné z: http://www.phoenixtm.com/assets/brochures/English/HTS02-V10.pdf

[39] PhoenixTM PTM1220: HT logger. In: *PhoenixTM* [online]. [cit. 2020-05-12]. Dostupné z: http://www.phoenixtm.com/assets/Uploads/products/logger/ht-logger.jpg

List of the used symbols and abbreviations

em	Electro magnetic
v	Electromagnetic radiation velocity
μ	Permeability
ϵ	Permittivity
μ_0	Permeability in vacuum
ϵ_0	Permittivity in vacuum
Q	Total radiated energy
Q_a	Absorbed energy
Q_r	Reflected energy
Q_t	Transmitted energy
a	Absorption power
r	Reflection power
t	Transmission power
λ	Wavelength
bb	Black body
m_0	Invariant mass
E	energy
h	Planck constant
f	Frequency
p	Momentum
c	Speed of light
ω	Angular frequency
ħ	Reduced Planck's constant
B-E	Bose Einstein distribution
$n(\omega)$	the expected value of particles in an energy state for B-E
k	Boltzman constant
T	Absolute temperature in Kelvins
t	Temperature in °C
Γ	Volume of phase space
$g(E)$	Density degeneration
$\rho(w)$	Energy density
S	Entropy
ε	Emissivity
$H(T)$	Radiation intensity
$\alpha(T)$	Absorbtion
λ_p	Peak wavelength
ε_r	Emissvity of real object
I_λ	Intensity of real object
$I_{\lambda b}$	Intensity of bb
R	Resistance
R_0	Referencing electrical resistance
α, β, γ	Material constants
RTD	Resistance temperature devices
T_{REF}	Reference temeperature
EMF	Electromotive Force
V	Potential
V_c	Contact potential

n_L Left higher density
n_R Right lower density
Π_A , Π_B Peltier coefficients
J Current density
K_1 Thompson´s First coefficient
K_2 Thompson´s Second coefficient
S_B Seebeck coefficient
SB Stefan-Boltzman
SPU Signal processing unit
TIR Thermal imaging camera
T160 Thermal camera TIM 160
TC TIM Connect software
MS09 Pyrometer Metis MS09
T In experimental part is used *T* as temperature in °C
t In experimental part is used *t* as time
P_L/R Left and right pyrometers measuring a tube after heating
T_L/R Thermal camera that measuring left and right side of the tube before pressing
UP_L/R Pyrometer that measuring left and right side of the tube before pressing